Formulation development, characterization & stability studies

4. FORMULATION, DEVELOPMENT, CHARACTERIZATION AND STABILITY STUDIES

Introduction

In the present scenario, nanocarrier drug delivery systems are emerging as a novel tool to deal with some of the major disease such as cancer. More and more nanocarrier based anti-cancer drug formulations are being introduced in the market with advanced strategic modification and enhanced therapeutic benefit based on localization of these nano-carriers due to enhanced permeation and retention (EPR effect). The rationale behind association of drugs with colloidal carriers such as nanoparticle, liposome or micelles used for targeted drug delivery, long circulation half life, to reduce side effect, prevent from degradation or reversal of MDR. NPs of biodegradable polymers can provide a way of sustained, controlled and targeted drug delivery to improve the therapeutic effects and reduce the side effects of the formulated drugs. Poly(D,L-lactide-co-glycolide) (PLGA) and poly (n-butyl cyanoacrylate) (PBCA) are widely used as polymeric carriers for preparation of NPs. Both materials are very for its property such as biocompatibility, biodegradability and widely accepted for human use (chaudhari et al, 2010; shah et al, 2009).

PLGA is a copolymer of lactic acid and glycolic acid. Depending on the ratio of lactide to glycolide, different forms of PLGA can be obtained, which are usually identified with regard to the monomers ratio used (e.g., PLGA 75:25 identifies as 75% lactic acid and 25% glycolic acid). PLGA is one of the most successfully used biodegradable polymers for the development of nanomedicines because it undergoes hydrolysis in the body to produce the biodegradable metabolite monomers, lactic acid and glycolic acid, which are effectively processed by the body, resulting in minimal systemic toxicity (Wu, 1995). The degradation rate of PLGA depends on the molar ratio of lactic and glycolic acids in the polymer chain, molecular weight of polymer, the degree of crystallinity and the glass transition temperature (Tg) of the polymer. By manipulating the molecular weight and lactide/glycolide ratio, the degradation time of PLGA and, subsequently, the release profile can be varied accordingly (Lu et al, 2009). Many approaches are proposed for the preparation of PLGA particles. The emulsification-evaporation method, the spontaneous

emulsification-solvent diffusion method (SESD) (Bilati et al, 2005), the nanoprecipitation method (Rivera et al, 2005) and the spray-drying method (Cheng et al, 2008) are all widely used in preparing PLGA nano/microparticles of various size.

A wide variety of therapeutic agents, including low-molecular-weight lipophilic or hydrophilic drugs, high-molecular-weight DNA or antisense DNA, can be encapsulated inside NPs. The entrapped moiety in the polymeric matrix of NPs is released at a sustained rate by diffusion or by degradation of the polymeric matrix (Parveen and Sahoo, 2008), thereby giving a sustained release formulation to elicit enhanced therapeutic efficacy. Thus, due to their nontoxic behaviour and excellent biocompatibility and biodegradability properties, PLGA NPs have been most extensively studied among all the commercially available polymers. Several studies have investigated the mechanism of intracellular drug delivery by PLGA NPs. It is generally thought that PLGA NPs are taken up by endocytosis, which then release the drug at intracellular locations. Many studies demonstrated rapid and efficient cellular uptake of PLGA NPs, based on microscopic observation of PLGA NPs encapsulating a fluorescent probe and/or measurement of the intracellular level of the probe (Sahoo et al, 2002; Panyam et al, 2002).

Nanocarriers must be hidden from the reticuloendothelial system (RES), which destroys any foreign material through opsonisation, followed by phagocytosis by macrophages. Intravenously injected NPs are mostly taken up by the macrophages present in the liver and the spleen within minutes of drug administration (Alexis et al, 2008). Different reports demonstrate that the rapid RES uptake of PLGA NPs could be significantly reduced by modifying their surface with poly(ethylene glycol) (PEG) (Gref et al, 1994). The most widely accepted theory for this increased circulation time is that PEG reduces the protein interactions on the surface by preventing opsonin binding (Owens and Peppas, 2006). PEG-modified PLGA NPs, prepared mostly by using a di-block copolymer of PLGA-b-PEG as an additive, prolonged their half-life considerably in the circulation due to the presence of highly mobile and flexible PEG chains on the surface.

4.2 PLGA Nanoparticle

4.2.1 Materials and Method

4.2.1.1 Materials

PLGA 502H, (lactide/glycolide ratio 50:50, inherent viscosity 0.22dl/g) was obtained as a gift sample from Boehringer Ingelheim, Germany. DTX and ZOL were obtained as a gift sample from Sun Pharma Advanced Research Company Ltd (SPARC), Vadodara, India. PEG bisamine (Mol wt. 3350 Da), CDI, NHS, DCC and 6-coumarin were purchased from Sigma Aldrich, India. Poloxamer 188 was kindly gifted by BASF, India. HCl, NaOH, SDS, DMF and DMSO were obtained from S. D. Fine Chemicals, India.

4.2.1.2 Synthesis and characterization of PLGA-PEG conjugate

PLGA-PEG conjugate was synthesized using N-Hydroxysuccinimide (NHS) and Dicyclohexylcarbodiimide (DCC) as an activator (Jayant Khandare and Tamara Minko, 2006). Carboxylic group of PLGA (1 gm) was activated by addition of NHS (8.6 mg) and DCC (15.5 mg) in distilled DMF (free from moisture) to form PLGA-NHS. The reaction mixture was allowed to stir in tightly closed flask under nitrogen blanket for 12 h. PLGA-NHS was then precipitated with addition of ice cold diethyl ether. Reaction mixture was filtered to collect precipitates. Precipitation process was repeated again to remove any remaining DCC impurity. Precipitate was redissolved in small quantity of acetone and this solution was precipitated twice in cold methanol to remove excess NHS. Residual methanol was then evaporated using rotary flask evaporator. Activated PLGA was dissolved in DMF followed by addition of PEG bisamine (670 mg) which allowed to react for 12 h. Reaction mixture was executed for dialysis for 36 h with change in medium at regular intervals to remove unreacted PEG bisamine and dialysed product was lyophilized (HetoDry, Germany). Lyophilised product was stored under refrigeration till further use. Each reaction step as well as purification step were monitored by TLC using 100% ethyl acetate as a mobile phase and iodine as a spotting reagent. The characterization of conjugate was performed by FTIR and NMR.

4.2.1.3 Synthesis and characterization of PLGA-PEG-ZOL conjugate

Conjugation of ZOL with PLGA-PEG-NH_2 was performed using N,N'-Carbonyldiimidazole (CDI) as a conjugation linker (Alila S. et al, 2009). In brief, ZOL (100 mg) was dissolved in distilled DMF with triethylamine (TEA). CDI (90 mg, moisture free) was added to that solution in tightly closed vessel under nitrogen blanket. The reaction mixture was allowed to react for 24 h at 60°C on oil bath with constant stirring. TEA was then evaporated on rotary flask evaporator to precipitate activated ZOL and separated by centrifugation. Precipitates are washed twice with acetonitrile to remove CDI and dried on rotary flask evaporator to obtain pure activated ZOL. PLGA-PEG (1gm) and activated ZOL (22.6 mg) were dissolved in DMSO with TEA in tightly closed vessel under nitrogen blanket and allowed to react for 12 h. The reaction mixture was dialyzed against distilled water for 24 h to remove excess activated ZOL with change of dialysis media at regular intervals. Colloidal solution from dialysis bag was collected and lyophilized for to obtain PLGA-PEG-ZOL conjugate. Lyophilised product was stored in refrigerated conditions till further use. Each reaction step as well as purification step were monitored by TLC using ethyl acetate with TEA (1-2 drops) as a mobile phase and iodine as a spotting reagent. The characterization of conjugate was performed by FTIR and NMR.

4.2.1.4 Preparation of PLGA NP

DTX loaded PLGA NPs were prepared by solvent diffusion (nanoprecipitation) technique as described by Fessi et al., 1989. The organic phase (acetone) containing DTX (7.5 mg) and PLGA (100 mg) were slowly injected (0.5mL/min) into 20 ml of aqueous phase containing Poloxamer 188 (0.5% w/v) as stabilizer on a magnetic stirrer (Remi Equipments, Mumbai) (figure 4.1). With the diffusion of solvent in to the aqueous phase, the polymer precipitates with entrapped DTX in polymer matrix, leading to formation of DTX loaded PLGA NPs. The resulting nanoparticle dispersion was further stirred to evaporate the organic phase under vacuum on rotary flask evaporator (Superfit Equipments, India). NPs were recovered by centrifugation for 30 min at 25,000 rpm (Sigma 3K30, Germany) washed three times with distilled water to remove excess surfactant, resuspended and then lyophilized for 48 h (Heto Drywinner, Denmark) using trehalose as a cryoprotectant. PLGA-PEG and PLGA-PEG-ZOL NPs were prepared in

same way by replacing PLGA with PLGA-PEG and PLGA-PEG-ZOL in a fixed molar ratio. 6-coumarin loaded nanoparticles were prepared in similar way with addition of 6-coumarin in place of DTX.

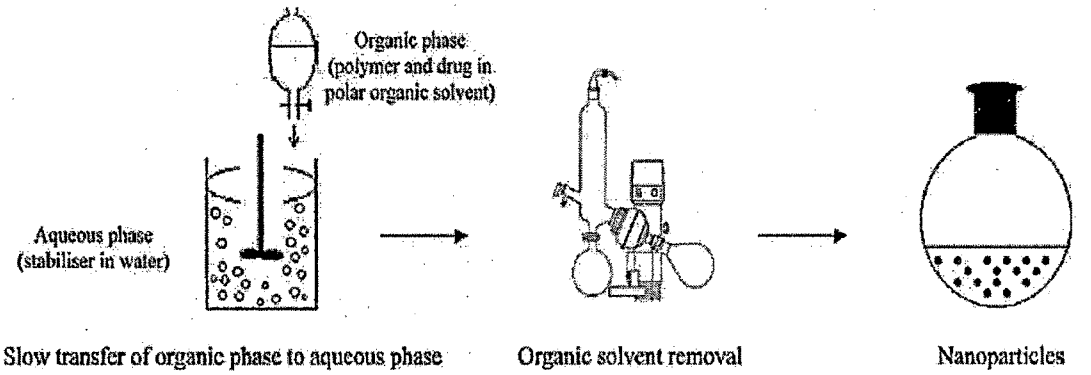

Figure 4.1: Preparation scheme of PLGA NP by solvent diffusion - nanoprecipitation method

4.2.1.5 Entrapment efficiency

Lyophilized NPs (5mg) were dissolved in 5ml acetonitrile. The content of DTX is estimated using reverse phase HPLC using C18 column, mobile phase Acetonitrle: water (70:30), 1 ml/min flow rate and 230 nm at UV detector (Shimadzu, Japan). The % entrapment efficiency was calculated as a ratio of the total entrapped DTX to the total amount of DTX used as below equation:

$$\%\text{Entrapment efficiency} = \frac{\text{Amount of Entrapped drug X 100}}{\text{Total added drug}}$$

4.2.1.6 Particle Size Analysis

The particle size (z-average) and poly dispersity index (PDI) of the nanoparticle was analyzed by photon correlation spectroscopy (PCS) using a Malvern Zetasizer Nano

(Malvern Instruments; UK). 0.2 mL of nanoparticle suspension was diluted to 1.0 mL with distilled water (DW) and measured after an equilibration time of 1 minute. The Zetasizer Nano is operating with a 4 mW He-Ne-Laser at 633 nm and non invasive back-scatter technique (NIBS) at a constant temperature of 25°C. The measurements were conducted in the manual mode. The size distribution by intensity and volume was calculated from the correlation function using the multiple narrow mode of the Dispersion Technology Software version 4.00 (Malvern, Herrenberg, Germany). Thereby, the resulting size distributions show the hydrodynamic diameter. The average particle size and PDI was calculated after performing the experiment in triplicate. PDI near to zero represents a homogenous particle population while near to 1.0 indicates a heterogeneous size distribution of the nanoparticle sample.

4.2.1.6 Zeta (ς) potential analysis

The zeta potential (ς potential) of the prepared nanoparticle was measured by microelectrophoresis using Malvern Zetasizer Nano ZS (Malvern, Instrument, U.K.). Zeta potential of the nanoparticle was measured after separation of the free drug from the nanoparticle. 0.2 mL of nanoparticle was diluted to 1 mL of DW. The determination of the zeta potential was realized at 25°C after injecting 1 mL of the sample into a standard sample cell.

4.2.1.7 In-vitro drug release of Docetaxel

Phosphate buffer solution (PBS, pH 7.4) with 10 % ethanol and 0.5% v/v tween 80 was selected as the drug release medium. Nanoparticle suspension transferred into a dialysis membrane (MW cut-off: 12000 Da, Himedia India). The dialysis bag was placed in 20 mL release medium. The release study was performed at 37°C on magnetic stirrer. At selected time intervals, 1 mL buffered solution from the receptor compartment was removed and replaced with 1 mL fresh buffer solution. The content of DTX is estimated using reverse phase HPLC using C18 column, mobile phase Acetonitrle: water (70:30), 1 ml/min flow rate and 230 nm at UV detector (Shimadzu, Japan).

4.2.1.8 In vitro release of 6-coumarin

In vitro release of 6-coumarin loaded PLGA NPs was carried out by same method as above. This study was conducted under light protection and samples were wrapped by aluminum foil. The released 6-coumarin was estimation by spectrofluorimetry at excitation and emission wavelength of 430 nm and 485 nm respectively.

4.2.1.9 Differential scanning calorimetry (DSC) studies

In order to investigate the possible interaction between the drug and exipients (polymer), differential scanning calorimetry (DSC) studies were carried out. DSC thermogram of the formulation was compared with the DSC thermogram of pure drug sample. About 2-5 mg of sample was heated, in a hermetically sealed aluminum pan, at a heating rate of 10° C/min, from 30° C to 250° C under a nitrogen atmosphere. An empty aluminum pan was used as the reference for all measurements.

4.2.1.10 FTIR studies

The sample was ground with a specially purified salt (potassium bromide) finely (to remove scattering effects from large crystals). This powder mixture is then pressed in a mechanical die press to form a translucent pellet. These pellets were used to take FTIR spectra.

4.2.1.11 NMR spectroscopy

The proton NMR spectrum of each conjugate was recorded to confirm formation of each conjugate. Each sample were dissolved in DMSO (deuterated, Merck Germany) and transferred to a 5 mm NMR tube. NMR tube containing sample was placed in 5 mm broad band probe head and pulse programming was performed using Brucker 300MHz (Switzerland) and the NMR spectra was recorded.

4.2.1.12 Cryo Transmission Electron Microscopy (TEM)

Cryo TEM is a microscopic technique whereby a beam of electrons is transmitted through an ultra thin specimen, interacting with the specimen as it passes through. An image is formed from the interaction of the electrons transmitted through the specimen, the image is magnified and focused onto an imaging device. Unlike TEM, cryo TEM

sample studied at cryogenic temperatures (generally liquid nitrogen temperatures) and allows the observation of specimens that have not been stained or fixed in any way, showing them in their native environment.

4.2.1.13 Estimation of PEG in NP

PEG total content in PEG-PLGA nanoparticles (% of the particles weight) was determined by a calorimetric method, taking advantage of the formation of a complex between PEG and iodine (Peracchia M.T., 1997). Practically, lyophilized nanoparticles (10 mg) were allowed to completely degrade in NaOH 2N, at 50 °C during four days. After neutralization with HCl 1N, 125 µl of I_2/KI solution was added to 5 ml of a diluted solution (1:100) of the degraded nanoparticles. Before lyophilization, nanoparticles were washed four times, in order to remove all the PEG free or weakly bound to the particles. The colorimetric absorption was conducted by spectrophotometric measurements at 500 nm. The PEG content was calculated using PEG standard calibration curve prepare from known concentration of PEG using above method.

4.2.1.14 Estimation of Residual poloxamer P188

Estimation of poloxamer P188 in final PLGA NP formulation is very important as the concentration of surfactant need to control up to permissible limit for i.v. injection. Determination of poloxamer P188 in final formulation was determined using colorimetric assay after color induction using ammonium ferroisothiocynate. The resulted solution was performed for absorbance at 510 nm in spectrophotometer.

4.2.1.15 Salt and Serum Induced Aggregation Studies

Colloidal stability of NPs was tested using salts such as sodium sulphate and calcium chloride which are well known as aggregation inducer. NPs were diluted with sodium sulphate (1 M) and calcium chloride (30 mM) solution and kept for fixed time interval under slow stirring. To evaluate the serum protein adsorption, NPs formulation was mixed with 1% fetal bovine serum (FBS) in phosphate buffer saline (PBS) in 1:10 proportion and kept with slow stirring. The average particle size was measured after fixed time interval to determine the salt and serum induced aggregation of NPs.

4.2.3.16 In vitro bone binding affinity assay

ZOL solution and PLGA-PEG-ZOL NPs were evaluated for *in vitro* bone binding affinity. Both samples having same amount of ZOL were diluted with 100 ml PBS and kept on slow stirring along with human bone powder. After each time point, 2 ml solution was withdrawn and centrifuge to separate bone powder. Amount of ZOL in bone powder was estimated after dissolving bone powder in 1 M HCl.

4.2.1.17 Selection of cryoprotectants for lyophilization of NPs

The major limitation of colloidal carriers is their instability i.e. they tend to agglomerate during storage particularly in liquid formulations that be caused due to a greater surface area of the system and the resulting thermodynamic instability that favors aggregation of colloidal particles. Hence do freeze drying of the liquid NPs formulations as it is one of the well established methods of preservation of unstable molecules over a long period of time. To the suspension of the optimized batch from the above studies, different cryoprotectants like sucrose, mannitol and trehalose were added in different concentrations before freeze-drying. The effect of these cryoprotectants at different cryoprotectant to nanoparticle ratios (1:1, 3:1 and 5:1) on the redispersibility of the freeze-dried formulations and the size of the nanoparticles before and after freeze-drying was investigated.

4.2.2 Stability studies

Stability is defined as the capacity of a drug substance or drug product to remain within established specifications to maintain its identity, strength, quality, and purity throughout the retest or expiration periods (ICH guideline, 2003). Stability testing provides evidence that the quality of a drug substance or drug product under the influence of various environmental factors changes with time (ICH Draft guidance, Stability Testing of New Drug Substances and Products, Q1A (R2), 2003). Nanoparticles have been extensively used to deliver a wide range of drugs as they can protect the drug from metabolizing enzymes, acidic degradation and also from oxidative degradation as in drug was remain in encapsulation or entrapped form which prevent exposure of drug. During preparation,

particulate delivery systems are lyophilized and, although compactly arranged, can be readily resuspended in aqueous media after being stored at 4°C. However, storage temperature is important in maintaining the integrity of these delivery systems.

In general, "significant change" for a drug product is defined as:

1. A 10% change in assay from its initial value;
2. Failure to meet the acceptance criteria for appearance, physical attributes, and functionality test (e.g., particles size, drug content and zeta potential)
3. Failure to meet the acceptance criteria for particle size growth.

4.2.2.1 Stability testing protocol

The stability studies were performed for the lyophilized nanoparticles. The samples were kept in transparent glass vials and stored at 5°C ± 3°C (in refrigerator) and at 25°C ± 2°C/60 ± 5%RH. At different time points the samples were withdrawn and were subjected to reconstitution properties, particle size, zeta potential and drug content studies. During sampling, the vials were visually examined for the evidence of any change in cake morphology and discoloration.

4.2.3 Result and discussion

4.2.3.1 Preparation and optimization of DTX loaded PLGA NPs

Nano-precipitation technique involves a spontaneous gradient-driven diffusion of water miscible organic solvents into the continuous aqueous phase. This process may apparently appear simple, but it may involve complex interfacial hydrodynamic phenomenon. Here the addition of acetonic solution of polymer and drug resulted in spontaneous emulsification of the oily solution in the form of nano-droplets. This occurs as a result of some kind of interface instability arising from rapid diffusion of the acetone across the interface and marked decrease in the interfacial tension. The origin of the mechanism of nanosphere formation could be explained in terms of interfacial turbulence between two unequilibrated liquid phases, involving flow, diffusion and surface processes (Marangoni effect). Davis and Rideal, 1962 suggested that the interfacial turbulence is caused by localized lowering of the interfacial tension where the oil phase

undergoes rapid and erratic pulsations each of which is quickly damped out by a viscous drag.

The molecular mechanism of interfacial turbulence could be explained by the continuous formation of eddies of solvent (e.g. acetone) at the interface. Such eddies originate either during drop formation or in thermal inequality in the system. Thus, once the process has started, movements associated with previous kicks change the pressure inside the solvent by increasing the surface pressure inside the solvent or decreasing the interfacial tension. Thus, if the solvent droplets formed contain polymer, these will tend to aggregate and form nanoparticles because of continuous diffusion of solvents and because of the presence of a non-solvent medium (Guerrero et al., 1998). Among various factors, solute transfer out of the phase of higher viscosity, concentration gradients near the interface and interfacial tension sensitive to solute concentration are the most important factors. The presence of surfactant may markedly complicate the situation since they act to suppress interfacial flow and the rapid diffusion of acetone to the aqueous phase. The main advantage of surfactants in process is the instantaneous and reproducible formation of nanometric, monodispersed nanospheres exhibiting a high drug loading capacity (Fessi et al., 1989; Derakhshandeh et al., 2007).

4.2.3.2 Selection of surfactant for NP preparation

It was observed that the NPs shown reduced particle size and more stable when Poloxamer 188 was used instead of Poloxamer 407 as a steric stabilizer (table 4.1). For selection of stabilizer it was necessary to investigate reconstitution property and solid state stability. Non-ionic surfactants (poloxamer 188 and 407) provide steric repulsion between the particles causing a reduction in surface tension of the particles resulting in lower particle size (Behan et al., 2001; Huang et al., 2007). After reconstitution study it was found that poloxamer 188 readily reconstituted while poloxamer 407 show lump formation. Size increase on storage also found significantly high with poloxamer 407.

Table 4.1: Selection of surfactant on particle size and reconstitution property (Data: Mean ±SEM, n = 3)

	PVA	Poloxamer P188	Poloxamer P407
Particle Size (nM)	168 ±4.56	136 ± 3.75	147 ± 4.36
Reconstitution	lump formation	Uniform reconst.	Few Aggregates
Particle size after recon. (nM)	194 ± 5.43	145 ± 4.28	183 ± 5.49

Note: other parameter: surfactant concentration 1% w/v, organic to aqu ratio 1:2 and polymer conc 1%.

4.2.3.3 Effect of Poloxamer 188 concentration on particle size and entrapment efficiency

With increase in poloxamer 188 concentrations the particle size of PLGA NPs was found to decreases up to certain limit (table 4.2). With further increase in concentration result as increase in particle size which may be attributed to the increased viscosity of the external phase that caused a decrease in net shear stress resulting in increased particle size (Budhian et al., 2007). The miscibility of acetone with aq. poloxamer 188 solution results in partitioning of poloxamer 188 into the polymeric part of the organic phase. More molecules of poloxamer 188 can be physically incorporated onto the NPs surface (Boury et al., 1995; Rodriguez et al., 2004). Hence a large number of hydroxyl groups extending into the medium could be hydrated forming a hydrated layer at the surface of NPs surface to hinder nanoparticle aggregation. Increase in poloxamer 188 concentration had a positive effect on entrapment efficiency. With increase in poloxamer 188 concentration, more molecules of poloxamer 188 would be adsorbed onto the surface of nanoparticles (poloxamer 188 effectively covers the surface of NPs) hence resulting in a decrease in porosity of the NPs and hence an increase in entrapment efficiency (Rizkalla et al., 2006). As the amount of surfactant increases there is a decrease in zeta potential. PLGA NPs prepared without any surfactant has a negative zeta potential of -26.19 ± 2.71 mV which tends to decrease as the amount of surfactant increases because the surfactant effectively shields the functional groups on the NPs surface that inturn shifts the shear plane outwards, resulting in a reduction of the zeta potential (Ballard et al., 1984).

Table 4.2: Effect of surfactant concentration on particle size, zeta potential and % entrapment efficiency (Data: Mean ±SEM, n = 3)

Conc of Poloxamer P188	Particle Size (nM)	Zeta Potential (mV)	% Entrapment efficiency
0	148 ± 4.37	-26.19 ± 2.71	57.43 ± 2.37
0.5	134 ± 3.48	-23.42 ± 2.46	63.56 ± 2.29
1	136 ± 3.75	-16.53 ± 2.13	64.53 ± 2.43
2	162 ± 5.34	-11.74 ± 1.76	66.82 ± 2.50

4.2.3.4 Effect of Organic: aqueous phase volume ratio on particle size and entrapment efficiency

Aqueous to organic phase volume ratio was found to have a profound effect on particle size and entrapment efficiency. As the ratio was increased, the particle size and entrapment were increased (table 4.3). This can be attributed to faster solvent evaporation and faster polymer precipitation at higher ratios which leads to formation of less porous NPs. The more porous structure provides more mobility to the polymer chains and allows water to plasticize the polymer chains. This leads to an increase in particle size at lower ratios (Hyvonen et al., 2005). As the ratio decrease the entrapment decreases because the evaporation rate of solvent is less and the drug diffuses into the aqueous phase and also the viscosity of the organic phase is less at lower ratios. Hence the droplet size formed before precipitation is smaller resulting lower entrapment efficiency (Chorny et al., 2002, Song et al., 2008).

Table 4.3: Effect of organic to aqueous ratio on particle size and entrapment efficiency (Data: Mean ±SEM, n = 3)

Aqueous to Organic ratio →	2.0	2.5	3.0
Particle Size	127 ± 3.51	131 ±4.5	148 ± 5.74
% Entrapment Efficiency	64.36 ± 2.13	73.53 ± 3.43	72.97 ± 3.81

4.2.3.5 Effect of polymer concentration on particle size and entrapment efficiency

PLGA concentration had a positive effect on particle size i.e. a dramatic increase in particle size was observed that can be attributed to increase in viscosity of the organic phase which led to a reduction in net shear stress and promoting the formation of droplets with larger size (table 4.4). Also the increased viscosity of the organic phase would hinder rapid dispersion of PLGA solution into the aqueous phase resulting in larger droplets. These large droplets would form larger NPs as the solvent evaporates (Govender et al., 2000; Chorny et al., 2002). In addition, as the polymer concentration increases the amount needed of poloxamer (stabilizer) that is insufficient to cover the surface of droplets completely resulting in coalescence of droplets during solvent evaporation and hence aggregation of NPs occurs with a resulting increase in the hydrodyanamic diameter of the NPs.

Increase in PLGA concentration also increased the entrapment efficiency of DTX probably due to the increased viscosity of the solution resulting in increase in drug's diffusional resistance into the aqueous phase and thus enhance the entrapment efficiency of DTX in NPs (Song et al., 2008a). Additionally, the increase of particle size may be relevant to the increase of drugs entrapment efficiencies (Budhian et al., 2007). The increase of nanoparticles size with the increasing PLGA concentration can increase the length of diffusional pathways of drugs from the organic phase to the aqueous phase, thereby reducing the drug loss through diffusion and increasing the drugs entrapment efficiencies (Song et al., 2008b). As the polymer concentration increases there is an increase in the zeta potential towards the negative side because of the improperly shielded functional groups on the surface.

Table 4.4: Effect of PLGA concentration on particle size and % entrapment efficiency (Data: Mean ±SEM, n = 3)

PLGA conc (%w/v) →	**1.00**	**1.25**	**1.50**
Particle size	126 ± 4.63	132 ± 4.37	156 ± 6.29
% Entrapment Efficiency	61.48 ± 3.28	73.53 ± 3.43	75.16 ± 4.06

4.2.3.6 Estimation of PEG content

One of the important parameters to be estimated the content of PEG in NP formulations to confirm conjugation as well as to determine its amount in final formulation. Content of PEG was determined using I_2/KI based colorimetric method. The amount obtained was shown in table no 4.5. The amount estimated is very similar with the amount added in NP formulations.

Table 4.5: Estimation of PEG content in formulation (Data: Mean ±SEM, n = 3)

Formulation	% w/w of PEG added	Estimated PEG
PLGA NPs	0	--
PLGA-PEG10 NPs	10	9.62 ± 0.62
PLGA-PEG20 NPs	20	19.29 ± 0.83
PLGA-PEG30 NPs	30	30.48 ± 1.18
PLGA-PEG-ZOL NPs	20	18.83 ± 1.48

4.2.3.7 Estimation of residual amount of poloxamer P188

After washing step the residual amount of poloxamer P188 was estimated in each formulation. Result found that nonPEGylated formulation PLGA NP having highest residual poloxamer P188 concentration. It can be assume that the surface active agent attach on interface and difficult to remove after washing. The estimated residual amount is shown in table 4.6 in final lyophilized formulation.

Table 4.6: Estimation of poloxamer P188 in formulation (Data: Mean ±SEM, n = 3)

Formulation	Poloxamer P188 added (% w/v)	Residual Poloxamer P188 added (% w/v)
PLGA NPs	0.5	0.34 ± 0.052
PLGA-PEG10 NPs	0.1	0.31 ± 0.066
PLGA-PEG20 NPs	0.1	0.18 ± 0.037
PLGA-PEG30 NPs	0.1	0.17 ± 0.042

PLGA-PEG-ZOL NPs	0.1	0.12 ± 0.031

4.2.3.8 Characterization of DTX loaded NPs

The optimized batches of DTX loaded PLGA NPs (amount of PLGA 100mg, 0.5 % w/v poloxamer 188 and 2.5 as the ratio of aqueous to organic phase), PEGylated PLGA NPs and ZOL conjugated DTX loaded PEGylated PLGA NPs were characterized for particle size, entrapment efficiency and zeta potential as shown in table no 4.7 and figure 4.2. NPs demonstrated a mean hydrodynamic diameter below 150 nm with a polydispersity index of below 0.1 suggesting a uniform particle size distribution. Result demonstrates that with increase in PEG content Particle size decrease with increase in entrapment due to micellar stabilization. PEG give amphiphilic nature and form micelle as a result particle size decrease with increase in % drug entrapment. Due to shielding of surface function group by PEG there is decrease in zeta potential. Conjugation reaction shows no change in the mean particle size of NPs. The EE (%) was found to be 73.53 ± 3.43 % in case of unconjugated NPs and PEGylated PLGA NPs exhibited a slight increase in entrapment efficiency where as ZOL conjugated NPs had an entrapment efficiency of 75.73 ± 4.38 % attributed to the loss of surface drug fractions during incubation and conjugation purpose. The zeta potential of ZOL conjugated nanoparticles was slightly more negative than unconjugated ones that can be attributed to charge contributed by ZOL. PEGylation of PLGA NP shows decrease in zeta potential due to charge shielding by PEG.

Table 4.7: Physicochemical characterization of PLGA NP, PEGylated PLGA NP and ZOL conjugated PEGylated PLGA NP (Data: Mean ±SEM, n = 3)

Formulation	Particle size (nm)	Zeta potential (mV)	% Drug Entrapment	% Drug loading
PLGA NPs	132 ±4.5	-23.42 ± 2.46	73.53 ± 3.43	5.51
PLGA-PEG10 NPs	124 ±5.2	-15.85 ± 2.29	75.62 ± 4.10	5.67
PLGA-PEG20 NPs	113 ±5.4	-4.38 ±1.24	78.84 ± 3.27	5.91
PLGA-PEG30 NPs	110 ±6.3	-3.57 ±1.06	77.36 ± 3.40	5.80

PLGA-PEG-ZOL NPs	115 ±5.8	-26.33 ±3.15	75.73 ± 4.38	5.68

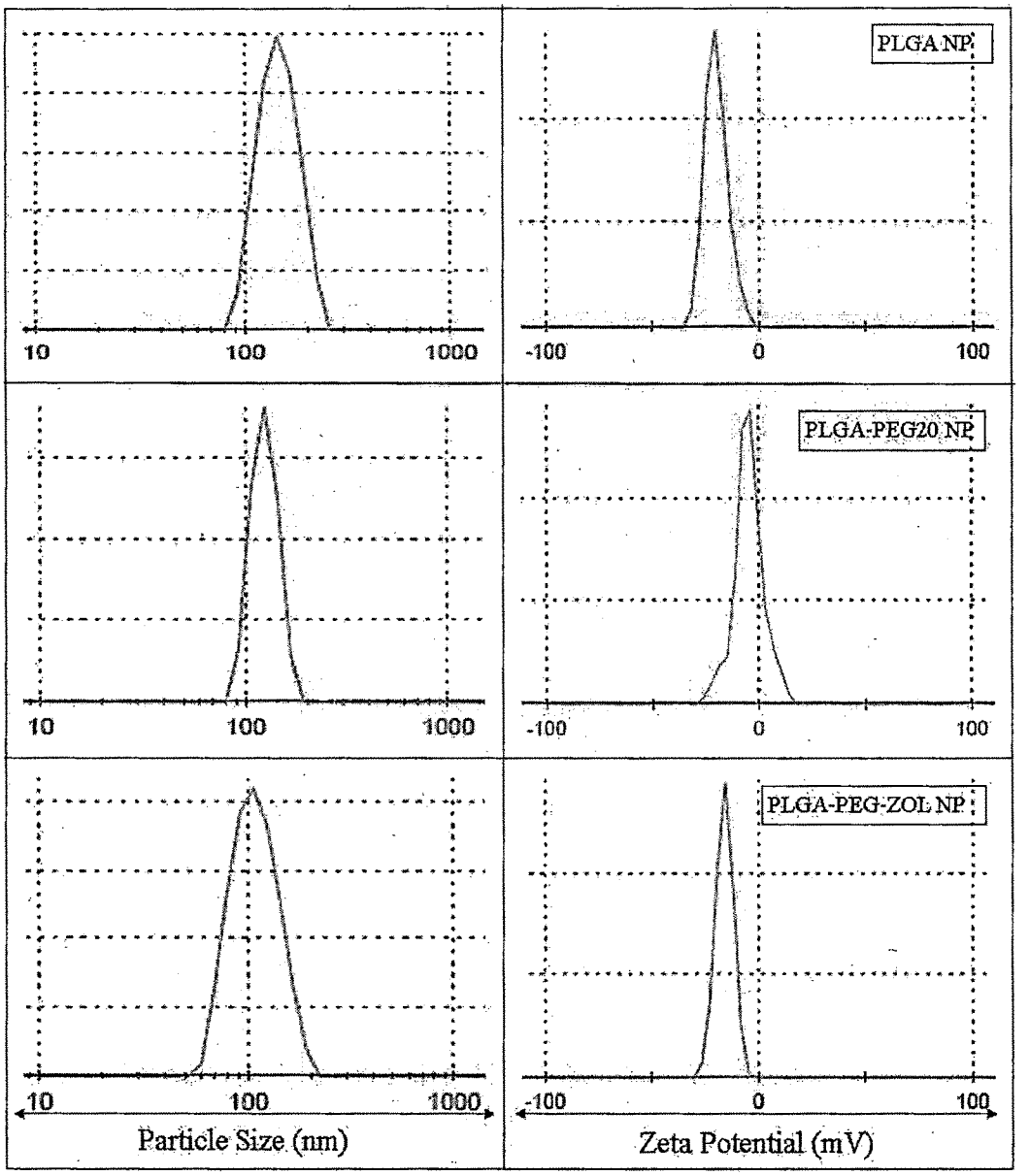

Figure 4.2: Particle size and zeta potential measurement reports of PLGA NP, PLGA-PEG20 NP and PLGA-PEG-ZOL NP (Data: Mean ±SEM, n = 3)

4.2.3.9 6-coumarin loaded PLGA NPs

Particles labeled with fluorescent dyes are frequently used to study cellular uptake quantitatively using a microplate reader and qualitatively by fluorescence/confocal

microscopy. 6-coumarin is a lipophilic fluorescent dye that is encapsulated in NPs for intracellular uptake studies. The major advantage of it is its high fluorescence even at low dye loading in NPs. 6-coumarin release from PLGA NP was evaluated and show very low burst release at initial 6 h. Hence it can be assumed that the dye does not leach from the NPs during the experimental time frame and therefore the fluorescence seen in the cells is caused by NPs and not by the free dye. The particle size and entrapment efficiency for 6-coumarin loaded NPs are tabulated in Table 4.8.

Table 4.8: Particle size and % drug entrapment of 6-coumarin loaded PLGA NP formulations (Data: Mean ±SEM, n = 3)

Formulation	Particle size (nm)	% Drug Entrapment	% Burst release in 6 h
PLGA NPs	135 ± 5.4	67.27 ± 4.18	3.24 ± 0.49
PLGA-PEG10 NPs	126 ±6.3	72.34 ± 4.13	5.62 ± 0.63
PLGA-PEG20 NPs	117 ±6.8	74.41 ± 4.22	4.57 ± 0.71
PLGA-PEG30 NPs	109 ±7.1	73.63 ± 3.98	3.89 ± 0.57
PLGA-PEG-ZOL NPs	114 ±5.2	77.20 ± 4.75	4.23 ± 0.49

4.2.3.10 FTIR

The Fourier transform infrared spectra of the PLGA, PEG, PLGA-PEG and PLGA-PEG-ZOL were display in figure 4.3. A prominent peak at 1748 cm^{-1} corresponds to C=O (str) which represent characteristic peak of PLGA. Medium peak at 1670 cm^{-1} corresponds to C=O (str) was observed which display amide bond formation between PLGA and PEG. Similarly characteristic peak of ZOL also observed in PLGA-PEG-ZOL. These peaks indicate the complete conjugate formation with all functional groups related to its structure.

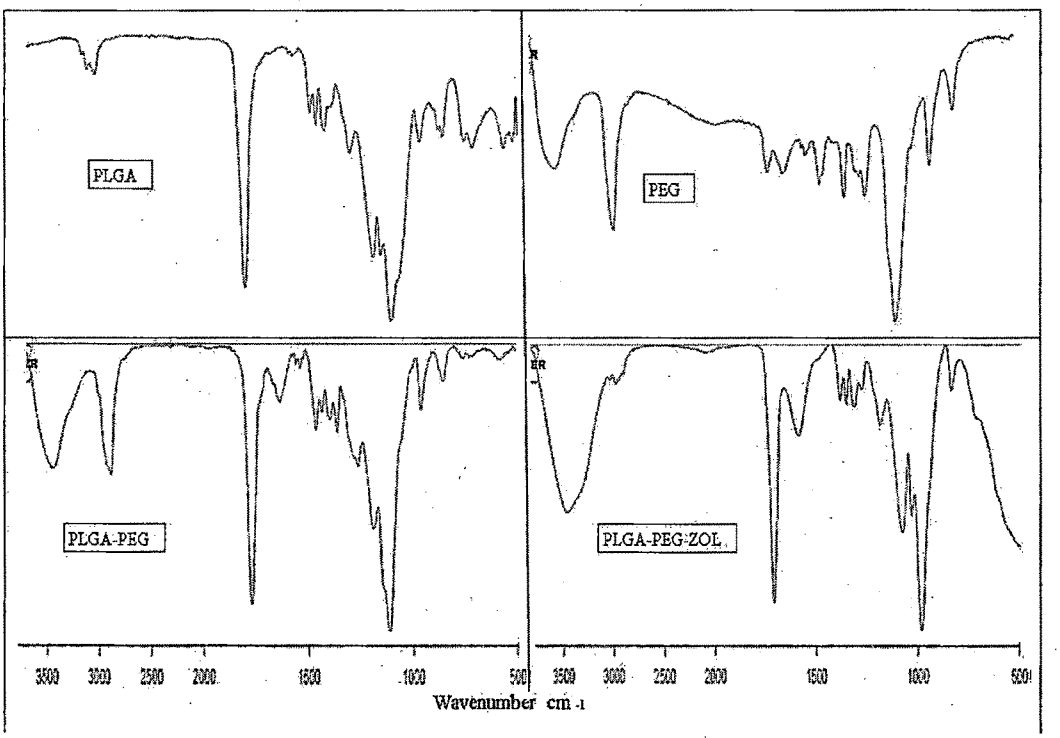

Figure 4.3: FTIR spectra of a) PLGA b) PEG c) PLGA-PEG and d) PLGA-PEG-ZOL

4.2.3.11 H^1 NMR spectroscopy

The H^1 NMR spectrum of PLGA-PEG-ZOL was given in figure 4.4. The characteristic peaks of lactide and glycolide at 4.9 ppm ($-CH_2-$) and 5.2 ppm (-CH-) were present in the conjugate. Strong peak at 3.5 ppm demonstrated presence of PEG ($-CH_2-O-CH_2-$). Characteristic peaks from zoledronate also confirm conjugation of PLGA-PEG-ZOL. Peak at 2.5 ppm arise because of solvent (H^2-DMSO) used to dissolve conjugate.

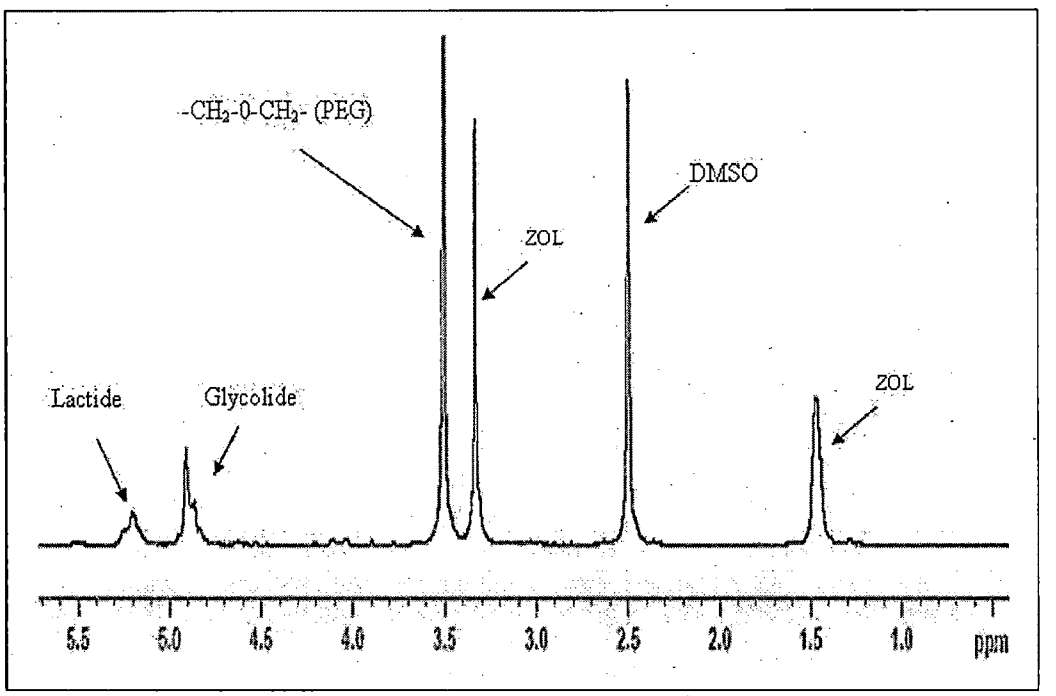

Figure 4.4: H^1 NMR spectrum of PLGA-PEG-ZOL

4.2.3.12 In-vitro drug release

PLGA degrades by hydrolysis of its ester linkages in the presence of water. In general the mechanism by which active agent is released from a delivery vehicle is a combination of diffusion of the active agent from the polymer matrices, bulk erosion of the polymer, swelling and degradation of the polymer. The degradation of PLGA is slow, therefore the release of DTX from NPs may depend on drug diffusion and PLGA surface and bulk erosion or swelling (Mu and Feng 2003). The curves of release of DTX from PLGA NPs depict a bi-phasic drug release (Figure 4.5). DTX release from NPs involved an initial rapid release phase followed by a lag phase of relatively slow release. A high initial burst was observed which can be attributed to the immediate dissolution and release of DTX adhered on the surface and located near the surface of the NPs (Magenheim et al., 1993). The initial burst for nanoparticles could be due to the diffusion release of drugs distributed at or just beneath the surface of the NPs. Then release is mainly due to the diffusion of drug molecules through the polymeric matrix of the NPs afterwards, the

matrix material would require time to erode in the aqueous environment, and then the release mechanisms of surface release and polymer erosion might be the main causes of the release behavior (Esmaeili et al., 2008). 98 % of the drug is released within 3 h in case of DTX solution. About 57.1 % of the drug is released in 5 days for PEGylated PLGA NP and ZOL conjugated NPs the drug release after 5 days was found to 61.8 %.

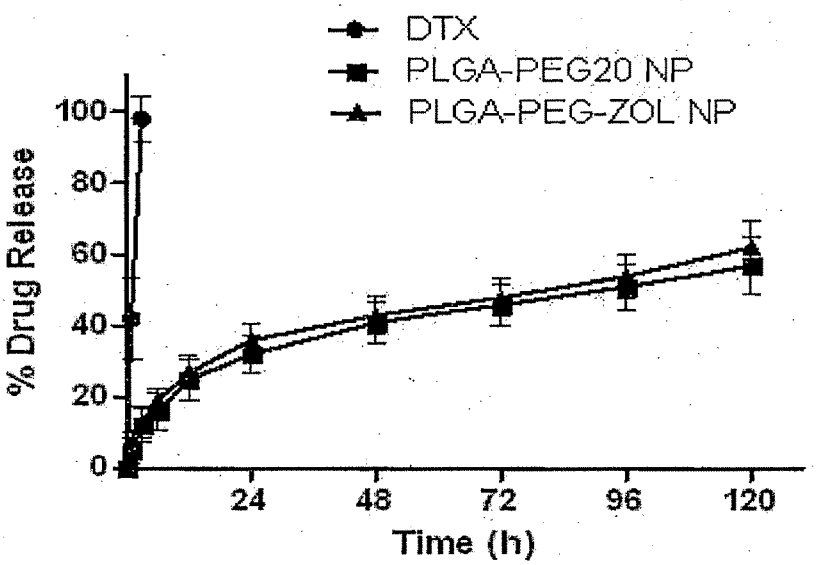

Figure 4.5: In-vitro release of DTX in pH 7.4 PBS containing 0.5 % tween 80 and 10% ethanol (Data: Mean ±SEM, n = 3)

4.2.3.13 DSC studies

DSC thermograms demonstrated that only pure DTX had an endothermic peak of melting at 200°C (aprox) whereas control or drug-loaded NPs had no such peak in the range 150-250 °C (Figure 4.6). The results thus indicate that DTX encapsulated in NPs is in the amorphous or disordered-crystalline phase of a molecular dispersion or in the solid-state solubilized form in the polymer matrix of NPs after fabrication (Mu and Feng, 2002, Esmaeili et al., 2008).

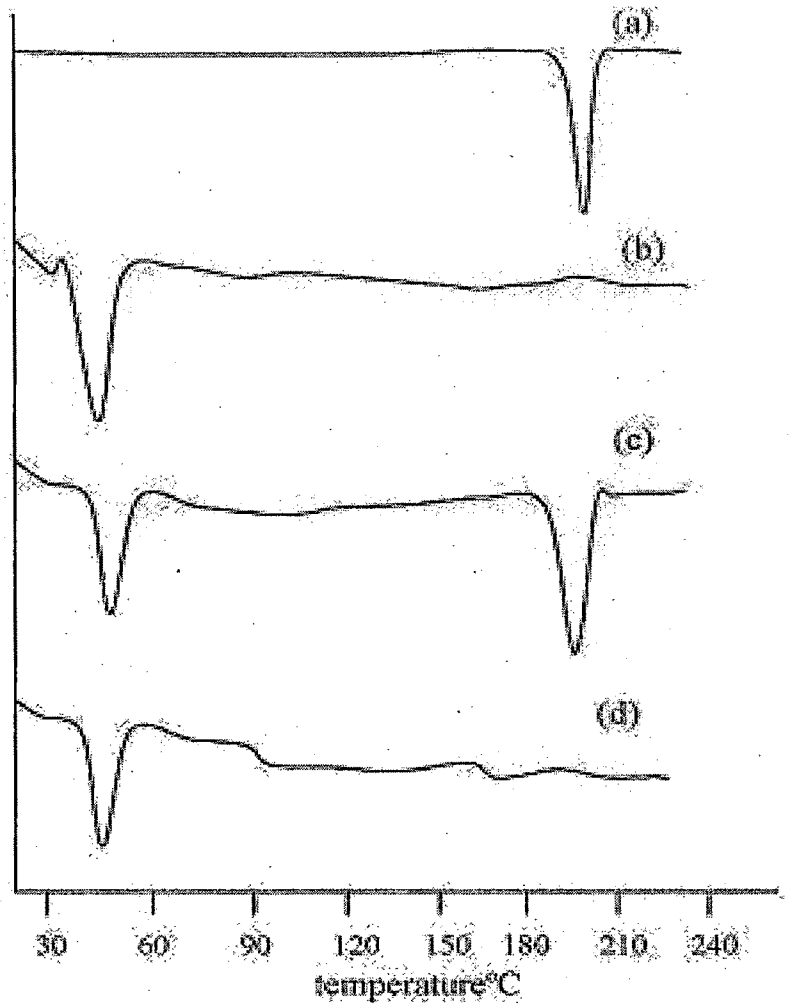

Figure 4.6: DSC study of (a) DTX, (b) PLGA-PEG-ZOL, (c) Mixture of DTX and PLGA-PEG-ZOL and (d) DTX loaded PLGA-PEG-ZOL NP

4.2.3.14 Cryo Transmission Electron Microscopy (CryoTEM)

CryoTEM images of Conjugated (figure 4.7a) and unconjugated (figure 4.7b) PLGA nanoparticles reveal the spherical shape and smooth surface of the NPs. It confirms the particle size in the nanometric range. The spherical nature of the NPs was not altered

after conjugation. The particle size measured in cryo TEM is very similar to particle size from zetasizer instrument.

a)

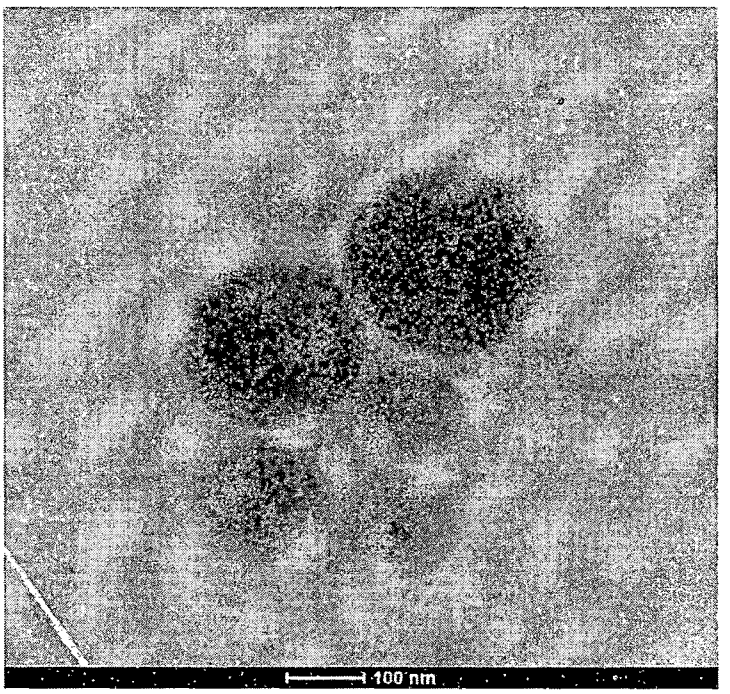

b)

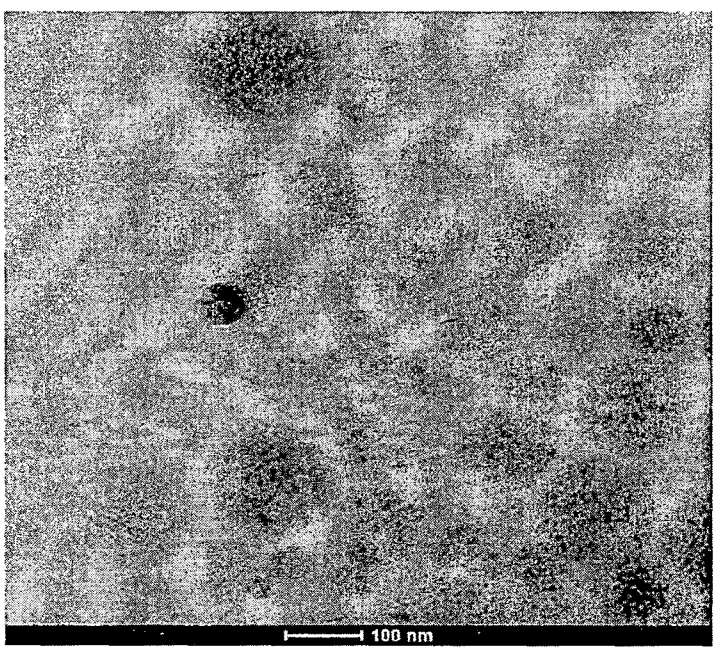

Figure 4.7: Cryo TEM images of PLGA NPs (a) unconjugated (b) ZOL- conjugated

4.2.3.15 Salt and serum induced colloidal stability studies

Aggregation resistance property of PEGylated and nonPEGylated PLGA NPs was determined using salt induced aggregation and serum induced aggregation methods. Results show that, among all formulations PLGA-PEG20 NPs and PLGA-PEG30 NPs displayed exceptionally high resistance to aggregation (Fig. 4.8a and b). The serum induced aggregation study showed that PLGA-PEG20 NPs and PLGA-PEG30 NPs did not show significant increase in particle size, while the particle size of PLGA-PEG10 NPs and PLGA NPs increased dramatically with time (Fig. 4.8c).

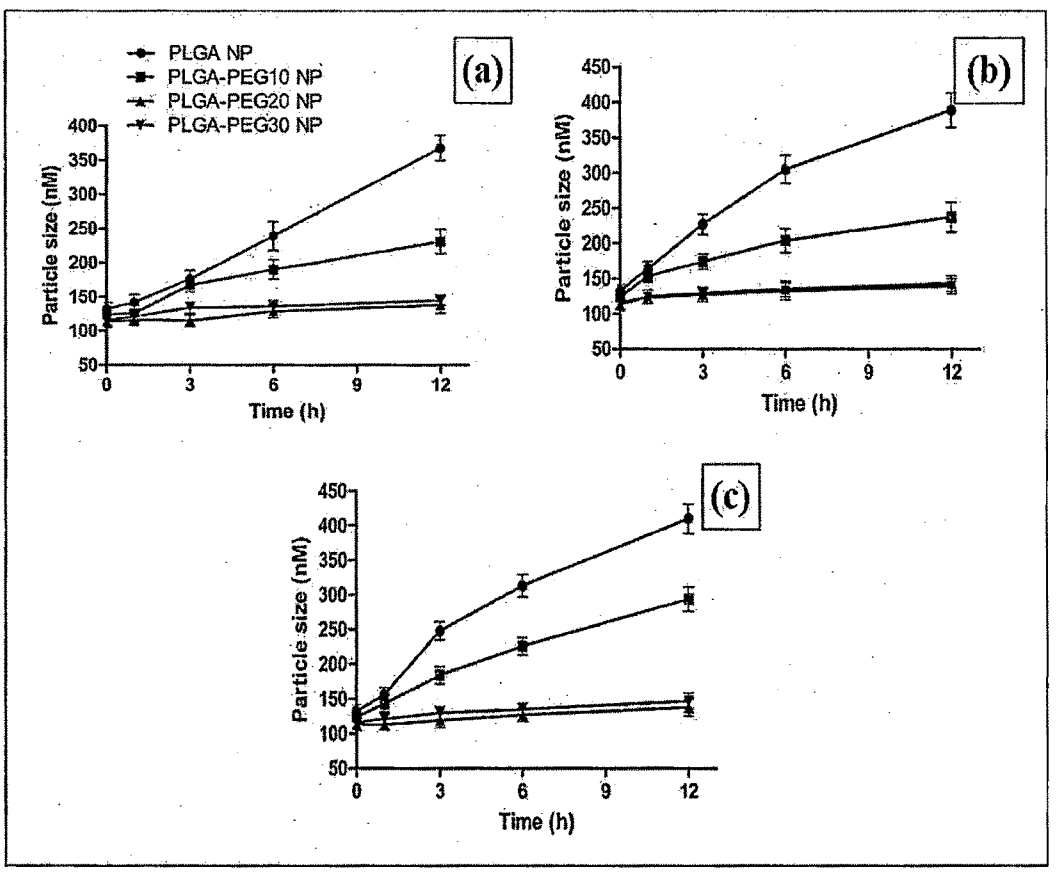

Figure 4.8.Colloidal stability studies using salt induced aggregation using (a): Na_2SO_4 and (b): $CaCl_2$. (c): Serum stability study of nanoparticulate formulations in PBS (pH 7.4) containing 1% FBS. (Data: Mean ±SEM, n = 3)

4.2.3.16 In vitro bone binding affinity assay

In vitro bone affinity study was carried out to evaluate bone binding property of zoledronic acid before and after conjugation with PLGA NP. Zoledronic acid found to have strong bone binding affinity. Figure 4.9 demonstrated that more than 95% zoledronic acid was found with bone in bound form within 6 h. The affinity of zoledronic acid conjugated with PLGA NP also found only slight difference to free zoledronic acid. After 6 h zoledronic acid conjugated PLGA NP shown more than 90% bone binding affinity.

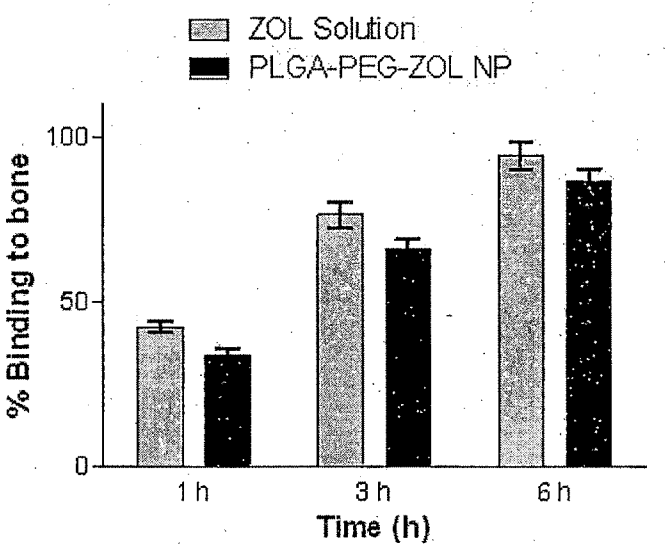

Figure 4.9: In vitro bone binding affinity of ZOL solution and PLGA-PEG-ZOL NP (Data: Mean ±SEM, n = 3)

4.2.3.17 Selection of cryoprotectants for lyophilization

Freeze-drying has been the most utilized drying method of nanoparticle suspensions. It is a promising way to increase chemical and physical stability of NPs over extended period of time. Transformation of the NPs suspension into a solid form will prevent Ostwlad ripening and avoid hydrolysis reaction. It is expected that solid state of lyophilizates would have a better chemical and physical stability than aqueous dispersions. Two important transformations occur during the process. The 1st is from aqueous dispersion to powder which involves freezing of the sample and evaporation of water under vacuum.

Freezing of the sample might cause instability due to the freezing out effects which results in changes of osmolarity and pH. The second transformation is resolubilization of the powder. Here at least in initial stages, situations arise which favor particle aggregation (low water and high particle content, high osmotic pressure). The protective effect of the surfactant can be compromised by lyophilization. After freeze drying, easy and rapid reconstitution and unchange particle size of the product are important features. In order to decrease NPs aggregation and to obtain a dry product addition of cryoprotectors will be necessary. For nanoparticles carbohydrates have been perceived to be suitable cryoprotectants since they are chemically innocuous and can be easily vitrified during freezing. There are considerable differences in the cryoprotective abilities of different carbohydrates.

Cryoprotectants decrease the osmotic activity of water and crystallization and favor the glassy state of the frozen samples. They are space holders which prevent the contact between the discrete NPs. Furthermore, they interact with the polar head groups of the surfactants and serve as a kind of "pseudo hydration shell" (Mahnert and Mader, 2001). It could be expected that particle size would increase after lyophilization, because nanoparticles tend to aggregate during this process. If the aggregated particles do not separate during redispersion, then larger particle sizes will be measured. Cryoprotectant when present at the nanoparticle surface, protects the particles from aggregation and make sure the redispersion requires a minimum of energy, being attributed to the formation of a steric barrier between the particles during lyophilization or to a stabilization of the particle dispersion due to electrostatic repulsions (Quintanar-Guerrero et al., 1998; Vandervoort and Ludwig 2002). Typical cryoprotectors are sucrose, sorbitol, mannitol, lactose, glucose, trehalose. Carbohydrates like mannitol and lactose can separate from frozen solution in the form of crystalline phases (Franks, 1998) whereas glucose and trehalose form amorphous masses at very temperatures (Saez et al., 2000).

Table 4.9 : Effect of different cryoprotectants on the particle size and redispersion (Data: Mean ±SEM, n = 3)

Cryoprotect	NPs:	Particle size (nm)	Reconstitut	Redispersibility

ant (CP)	CP	Before	After	ion time (sec)	
None	1:0		--	--	lump formation
Sucrose	1:1		--	--	lump formation
	1:3		246 ± 12.4	210	high aggregates
	1:5		219 ±9.6	150	few aggregates
Mannitol	1:1	130	--	--	lump formation
	1:3	±5.1	221 ± 10.7	140	few aggregates
	1:5		184 ± 9.3	100	clear solution
Trehalose	1:1		192 ± 10.2	110	few aggregates
	1:3		164 ± 6.4	90	clear solution
	1:5		137 ± 4.3	60	clear solution

The optimized batch of nanoparticles was lyophilized using different concentrations of sucrose, mannitol and trehalose. The redispersibility of the freeze-dried formulations and particle size of the nanoparticles before and after freeze-drying was measured and recorded in Table 4.9. Significant increase in particle size was measured in the absence of cryoprotectant. Sucrose was not effective cryoprotectant at any concentration. Reconstitution of NPs to which sucrose was added was more difficult compared to other formulations because of the sticky nature of the freeze dried cake, while NPs with other cryoprotectant showed a fluffy porous cake after freeze drying. Sameti et al., 2003 have reported that after freeze drying, residues appeared voluminous and snow like for trehalose and mannitol. Mannitol gave a good redispersiblity at NPs: CP ratio of 1:5 but the particle size was very high. Mannitol is known to show polymorphism and has a strong tendency to crystallize (Yu et al., 1998). Trehalose at 5 times w.r.t the total solid content was found to be optimum to be added during freeze drying for preserving the particle size of the NPs. The cryoprotective effect was attributed to the ability of the sugar additive to form a glassy amorphous matrix around the particles, preventing the particles from sticking together during removal of water (Konan et al., 2002). Hence

trehalose was found to be the best as a cryoprotectant to preserve the initial properties of NPs suspension after freeze drying.

4.2.4 Stability study

The stability studies were carried out according to ICH guidelines for drug substances intended for storage in a refrigerator. The long term stability study of lyophilized NPs was carried out at 5°C ± 3°C for six months. The nanoparticles short term stability was conducted for three months at 25 ± 2°C/60 ± 5% RH. Sampling was done at 0.5, 1, 2, 3 and 6 months. The stability profiles are shown in Tables 4.10.

It can be observed that when stored at 5°C ± 3°C, NPs are stable up to a period of six months with no significant change in either particle size, zeta potential or the drug content. The short term studies also indicate that nanoparticle formulation when stored at 25 ± 2°C/60 ± 5% RH are also stable with no significant change in drug content. All the samples stored at 5°C ± 3°C and 25 ± 2°C/60 ± 5% RH were redispersed easily within 2 minutes.

Hence, it can be concluded that the NPs should be stored at 5°C ± 3°C for maximum stability and a long term stability study is necessary for determining the optimum storage conditions for the lyophilized NPs.

Table 4.10: Stability data for ZOL conjugated DTX loaded PLGA-PEG NPs (Data: Mean ±SEM, n = 3)

Time	Particle size (nm)	Zeta potential (mV)	Drug content (%)	Reconstitution time (sec)	Reconstitution property
Initial	115 ± 5.4	-24.72 ± 2.28	100	50	Clear solution
5°C ± 3°C					
0.5	117 ± 6.5	-25.32 ± 2.34	98.4 ± 1.84	50	Clear solution
1	120 ± 5.6	-24.15 ± 3.02	98.1 ± 2.51	50	Clear solution

2	126 ± 5.2	-26.73 ± 2.58	96.7 ± 2.65	60	Clear solution
3	129 ± 6.0	-23.18 ± 2.23	97.1 ± 2.49	80	Clear solution
6	135 ± 7.3	-23.54 ± 2.16	95.9 ± 2.56	90	Clear solution
25 ± 2°C/60 ± 5% RH					
0.5	122 ± 4.8	-24.56 ± 2.43	98.1 ± 2.64	60	Clear solution
1	126 ± 6.0	-25.25 ± 2.21	97.2 ± 2.47	80	Clear solution
2	135 ± 7.3	-25.37 ± 2.98	96.2 ± 1.76	90	Clear solution
3	146 ± 7.2	-23.02 ± 3.17	95.3 ± 2.89	110	Clear solution

4.2.5 Conclusion

We can conclude that DTX can be effectively loaded into PLGA polymeric carriers and a particle size suitable for parenteral administration can be obtained. PEGylation and ZOL conjugation of PLGA NPs can be done effectively without significant change in morphology of the NPs. DTX entrapped PLGA NP formulation demonstrated a sustained release effect. PLGA based NP formulations found good stability while storage condition was refrigerated (2 - 8°C).

4.3 PBCA Nanoparticle

4.3.1 Introduction

The poly(butylcyanoacrylate) (PBCA) NPs have recently gained increasing interest in targeting and drug delivery, because of the ease of synthesis, biodegradability, ability to alter biodistribution of drugs and lower toxicity. PBCA NP have also shown good encapsulation properties and ability to cross the blood-brain barrier which makes PBCA NPs ideal for cancer therapy, especially for brain tumors (Woods, 1996; Kreuter 1996). The PBCA NPs are reported as a novel tool to deal with resistant cancer because of its unique drug delivery mechanism. Drug loaded in PBCA NP forms ions pairs with degraded polymer products at the physiological pH and thus protects the drug from

getting efflexed out from intracellular domain by resistance mechanism of the P-glycoprotein, i.e. MDR-1 type (Hu, 1996; Colin de Verdiere 1997). PBCA NP are generally prepared from butyl cyano acrylate monomers by emulsion anionic polymerisation in an acidic aqueous solution of a colloidal stabilizer such as dextran 70000, polysorbates, and poloxamers. The polymerization is initiated by the hydroxyl ions of water, and elongation of the polymer chains occurs by an anionic polymerization mechanism. It has to be understood that the anionic polymerization of such a reactive monomer can be controlled in an aqueous medium. Inclusion of drug can be made during the polymerization process or by adsorption on the preformed nanoparticles. The length of the alkyl pendant governs degradation rates (Müller et al. 1990, 1992) and toxicity (Lherm et al. 1992; Kante et al. 1982) of poly(alkyl cyanoacrylate) nanoparticles, which decrease in the order methyl> ethyl> butyl/isobutyl> hexyl/isohexyl.

A method of direct NPs generation using alkyl cyanoacrylate monomers by in situ polymerization has become well known. This method first developed and reported by Couvreur in 1979 (Couvreur et al, 1979). The use of cyanoacrylates in drug delivery is increasing because of its inherent properties such as stability, biodegradability, biocompatibility and targetability (Pereverzeva et al, 2008; Gelperina et al. 2002; Pereverzeva et al., 2007). Several clinical trials have also reported good in vivo tolerance of NPs prepared from this material (Zhou et al, 2009). Still the biggest break through research which gains more attention toward the use of PBCA as nanocarrier is by the predominant activity against resistance cancer where PBCA NP found to improve efficiency of chemotherapy. The mechanism found is after adhesion to cell surface PBCA's biodegraded products form ion pair with drug and enhances cell internalization without getting efflux by P-glycoprotein (P-gp) transporters which are responsible for resistance formation in cancer (Vauthier et al, 2003). In spite of excellent research in this area, still several constrain associated with the use of PBCA NP preparation method e.g.: low NP concentration in single batch, particle aggregation, high susceptibility of reaction with present impurities, uncertainty and sensitivity of reaction progress which changes direction suddenly with slight change in surrounding environment and slow process of reinitiation-depolymerization-repolymerization which increase time of NP preparation. Toxicity of residual unreacted monomer, stabilizer added previously in monomer (sulfer

dioxide, p-toluene sulphonic acid etc.) and limitation of the number of FDA approved initiator-additives for monomer are also challenging issues.

Some major breakthrough necessary in PEGylation process are method with easy scalable with less processing time, batch to batch uniformity, and better yield without compromising with purity. The method of redox reaction found successful in producing PEGylated PBCA NP, but the increasing number of steps, toxic reaction additives hinder as a method of choice. PBCA have found suitable for in situ conjugation with molecule having basic group such as -OH, $-NH_2$ which work as an initiator template for polymerization in absence or reduce availability of hydroxyl ion from self-ionization of water (Peracchia et al, 1997a). There was some attempt made with Methoxy-PEG-OH (Peracchia, 1997b), but no attempt have been reported using PEG-amine even though it is well known that amine group could work as a stronger initiator of polymerization reaction. Methoxy-PEG-OH having low reactivity of -OH group which hindered the reaction progress and turns to aggregation due to slow reactivity. With the help of reactive amino-PEG, this problem can be solved and the single step in situ concurrent PEGylation with NP formation could be possible with slight changes in reported methods of PBCA NP formation.

4.3.2 Material and method

4.3.2.1 Materials

Butylcyanoacrylate monomer was obtained as a gift sample from Evobond, Tong Shen Enterprise, Taiwan. DTX was obtained as a gift sample from Sun Pharma Advanced Research Company Ltd (SPARC), Vadodara, India. Methoxy-PEG-amine, PEG bisamine (Mol wt. 3350 Da) and 6-coumarin were purchase from Sigma Aldrich, India. Poloxamer 188 was kindly gifted from BASF, India. HCl, NaOH, SDS, DMF, DMSO obtained from S. D. Fine Chemicals, India.

4.3.2.2 Conjugation of ZOL with PEG bisamine

Conjugation of ZOL with PEG bisamine was performed using N,N'-Carbonyldiimidazole (CDI) as a conjugation linker (Alila S. et al, 2009). In brief, ZOL (100 mg) was dissolved in distilled DMF with triethylamine (TEA). CDI (90 mg, moisture free) was added to that

solution in tightly closed vessel under nitrogen blanket. The reaction mixture was allowed to react for 24 h at 60°C on oil bath with constant stirring. TEA was evaporated on rotary flask evaporator to precipitate activated ZOL which separated by centrifugation. Precipitates were washed twice with acetonitrile to remove CDI and dried on rotary flask evaporator to obtain pure activated ZOL. PEG bisamine (1g) and activated ZOL (22.6 mg) were dissolved in DMSO with TEA in tightly closed vessel under nitrogen blanket and allowed to react for 12 h. Pure conjugate was separated using column chromatography using acetonitrile: methanol (1:1) with TEA as mobile phase. The conjugate solution was dried on rota evaporator and stored in refrigerated conditions till further use. Each reaction step as well as purification step were monitored by TLC using acetonitrile: methanol (1:1) with TEA (1-2 drops) as a mobile phase and iodine as a spotting reagent. The characterization of conjugate was performed by FTIR and NMR.

4.3.2.3 Preparation of PBCA NP

PBCA NPs were prepared by modified anionic polymerization technique described by Mitra and Lin with some modifications (Mitra and Lin, 2003). Briefly, NPs were prepared in an acidic polymerization medium (pH 1.5-3) containing poloxamer 188 as a stabilizer. Water used was double distilled, filtered through 0.22 μm filter (Millipore, India) and exhibit very low conductivity value. To the prepared aqueous acidic polymerization medium, monomer was added and probe sonicated for 2 min (100W, 80% amp) followed by constant magnetic stirring at 700 rpm at 4°C protected from light. The polymerization reaction was allowed to continue with stirring continuously for 5 h. pH of the polymerization medium was gradually increased up to pH 5 using 0.5 M NaOH to complete the reaction and stirring was continued for further 30 min. The NP suspension was then neutralized with 0.5 M sodium hydroxide, filtered through 0.4 μm filter (Millipore, India), separated by centrifugation (Sigma 3K30, Germany) and lyophilized (Heto Drywinner, Denmark) using trehalose as a cryoprotectant. In case of DTX and 6-coumarin loaded NPs, the respective material was dissolved in monomer before adding into polymerization media.

4.3.2.4 Preparation of PBCA-PEG NP and PBCA-PEG-ZOL NP

PBCA-PEG NPs were prepared in similar manner as in case of PBCA NP with addition of mPEGamine and PBCA-PEG-ZOL NP was prepared using ZOL-PEG-amine as initiator in acidic polymerization medium respectively. Amine group of PEG work as nucleophilic initiator of polymerization reaction and propagated by micellar emulsification process while later turn to nanoparticle formation.

4.3.2.5 Turbidimetric studies to monitor particle formation

The turbidity measurement of particle formation of PBCA NPs is based on the particle size and the corresponding turbidity of the dispersion. As the formation of nanoparticles is related to increase particle size with corresponding increase in turbidity of the suspension, this method would give a qualitative idea of the particle formation process. For particle formation study polymerization of the PBCA monomer was carried out by EP and DP technique at 25°C and the %Transmittance of the dispersion was monitored continuously in a UV-Visible spectrophotometer (UV 1700, Shimadzu, Japan) at 600 nm.

4.3.2.6 Entrapment efficiency

Lyophilized NPs (5mg) were dissolved in 5ml acetonitrile. The content of DTX is estimated using reverse phase HPLC using C18 column, mobile phase Acetonitrle: water (70:30), 1 ml/min flow rate and 230 nm at UV detector (Shimadzu, Japan). The % entrapment efficiency was calculated as a ratio of the total entrapped DTX to the total amount of DTX used.

$$\%\text{Entrapment efficiency} = \frac{\text{Amount of Entrapped drug X 100}}{\text{Total added drug}}$$

4.3.2.7 Particle Size Analysis

The particle size (z-average) and poly dispersity index (PDI) of the nanoparticle was analyzed by photon correlation spectroscopy (PCS) using a Malvern Zetasizer Nano (Malvern Instruments; UK). 0.2 mL of nanoparticle suspension was diluted to 1.0 mL with distilled water (DW) and measured after an equilibration time of 1 minute. The Zetasizer Nano is operating with a 4 mW He-Ne-Laser at 633 nm and non invasive back-scatter technique (NIBS) at a constant temperature of 25°C. The measurements were

conducted in the manual mode. The size distribution by intensity and volume was calculated from the correlation function using the multiple narrow mode of the Dispersion Technology Software version 4.00 (Malvern, Herrenberg, Germany). Thereby, the resulting size distributions show the hydrodynamic diameter. The average particle size and PDI was calculated after performing the experiment in triplicate. PDI of 0.0 represents a homogenous particle population while 1.0 indicates a heterogeneous size distribution of the nanoparticle sample.

4.3.2.8 Zeta (ς) potential analysis

The zeta potential (ς potential) of the prepared nanoparticle was measured by microelectrophoresis using Malvern Zetasizer Nano ZS (Malvern, Instrument, U.K.). Zeta potential of the nanoparticle was measured after separation of the free drug from the liposome. 0.2 mL of nanoparticle was diluted to 1 mL of DW. The determination of the zeta potential was realized at 25°C after injecting 1 mL of the sample into a standard sample cell.

4.3.2.9 In-vitro drug release of Docetaxel

Phosphate buffer solution (PBS, pH 7.4) with 10 % ethanol and 0.5% v/v tween 80 was selected as the drug release medium. Nanoparticle suspension transferred into a dialysis membrane (MW cut-off: 12000 Da, Himedia India). The dialysis bag was placed in 20 mL release medium. The release study was performed at 37°C on magnetic stirrer. At selected time intervals, 1 mL buffered solution from the receptor compartment was removed and replaced with 1 mL fresh buffer solution. The content of DTX is estimated using reverse phase HPLC using C18 column, mobile phase Acetonitrle: water (70:30), 1 ml/min flow rate and 230 nm at UV detector (Shimadzu, Japan).

4.3.2.10 In vitro release of 6-coumarin

In vitro release of 6-coumarin loaded PBCA NPs was carried out by same method as above. This study was conducted under light protection and samples were wrapped by aluminum foil. The released 6-coumarin was estimation by spectrofluorimetry at excitation and emission wavelength of 430 nm and 485 nm respectively.

4.3.2.11 FTIR studies

The sample was ground with a specially purified salt (usually potassium bromide) finely (to remove scattering effects from large crystals). This powder mixture is then pressed in a mechanical die press to form a translucent pellet. These pellets were used to take FTIR spectra.

4.3.2.13 H^1 NMR spectroscopy

The proton NMR spectrum of each conjugate was recorded to confirm formation of each conjugate. Each sample were dissolved in DMSO (deuterated, Merck Germany) and transferred to a 5 mm H^1 NMR tube. H^1 NMR tube containing sample was placed in 5 mm broad band probe head and pulse programming was performed using Brucker 300MHz (Switzerland) and the H^1 NMR spectra was recorded.

4.3.2.14 Differential scanning calorimetry (DSC) studies

In order to investigate the possible interaction between the drug and exipients (polymer), differential scanning calorimetry (DSC) studies were carried out. DSC thermogram of the formulation was compared with the DSC thermogram of pure drug sample. About 2-5 mg of sample was heated, in a hermetically sealed aluminum pan, at a heating rate of 10° C/min, from 30° C to 250° C under a nitrogen atmosphere. An empty aluminum pan was used as the reference for all measurements.

4.3.2.15 Molecular weight determination

Gel permeation chromatography was carried out to determine the molecular weights of the formed polymers. The molecular weights of BCA polymer was determined by gel permeation chromatography (GPC) equipped with a Waters 510 pump, 50, 10-3 and 10-4 °A Phenogel columns serially set (Phenomenex, USA) and a Waters 410 differential refractometer. The mobile phase was tetrahydrofuran (THF) at a flow rate of 1.0 ml/min. Purified polymer was dissolved in THF to the concentration of 2% (w/v) and 50 µl of it was injected to the system.

4.3.2.16 Cryo Transmission electron microscopy (TEM)

Cryo TEM is a microscopic technique whereby a beam of electrons is transmitted through an ultra thin specimen, interacting with the specimen as it passes through. An image is formed from the interaction of the electrons transmitted through the specimen, the image is magnified and focused onto an imaging device. Unlike TEM, cryo TEM sample studied at cryogenic temperatures (generally liquid nitrogen temperatures) and allows the observation of specimens that have not been stained or fixed in any way, showing them in their native environment.

4.3.2.17 Content of PEG in NP formulation

PEG total content in PEG-PBCA NP (% of the particles weight) was determined by a calorimetric method, taking advantage of the formation of a complex between PEG and iodine (Peracchia M.T., 1997). Practically, lyophilized nanoparticles (10 mg) were allowed to completely degrade in NaOH 2N, at 50 °C during four days. After neutralization with HCI 1N, 125 µl of I_2/KI solution was added to 5 ml of a diluted solution (1:100) of the degraded nanoparticles. Before lyophilization, nanoparticles were washed four times, in order to remove all the PEG free or weakly bound to the particles. The colorimetric absorption was conducted by spectrophotometric measurements at 500 nm. The PEG content was calculated using PEG standard calibration curve prepare from known concentration of PEG using above method.

4.3.2.18 Estimation of Residual poloxamer P188

Estimation of poloxamer P188 in final PBCA NP formulation is very important as the concentration of surfactant need to control up to permissible limit for i.v. injection. Determination of poloxamer P188 in final formulation was determined using colorimetric assay after color induction using ammonium ferroisothiocynate. The resulted solution was performed for absorbance at 510 nm in spectrophotometer.

4.3.2.19 Salt and Serum Induced Aggregation Studies

Colloidal stability of NPs was tested using salts such as sodium sulphate and calcium chloride which are well known as aggregation inducer. NPs were diluted with sodium sulphate (1 M) and calcium chloride (30 mM) solute on and kept for fixed time interval

under slow stirring and particle size was monitored. To evaluate serum protein adsorption, NP formulation were mixed with 1% FBS in PBS in 1:10 proportion and kept with slow stirring. After fixed time interval particle size was measured.

4.3.2.20 In vitro bone binding affinity assay

ZOL solution and PBCA-PEG-ZOL NPs were evaluated for *in vitro* bone binding affinity. Both samples having same amount of ZOL were diluted with 100 ml PBS and kept on slow stirring along with human bone powder. After each time point, 2 ml solution was withdrawn and centrifuge to separate bone powder. Amount of ZOL in bone powder was estimated after dissolving bone powder in 1 M HCl.

4.3.2.21 Selection of cryoprotectants for lyophilization

To the suspension of the optimized batch from the above studies, different cryoprotectants like sucrose, mannitol and trehalose were added in different concentrations before freeze-drying. The effect of these cryoprotectants at different ratios of cryoprotectant to nanoparticles (1:1, 3:1 and 5:1) on the cake appearance, redispersibility and particle size of the nanoparticles before and after freeze-drying was investigated.

4.3.3 Results and Discussion

4.3.3.1 PBCA NP formation and drug entrapment mechanism

The NP formation is by micellar emulsification process. After sonication the size of monomer globules reaches to 1 to 10 μm range and stable because of surfactant and/or presence of PEG (Figure 4.10b). The reactive amine group of PEG reaches to surface of the globule which resulted as initiation of reaction and polymerization reaction propagated with time (Figure 4.11). After growing up to an oligomer, some trace amount of inhibitor (ex. sulfer dioxide, methansulphonic acid, *p*-toluene sulphonic acid and cynoacrylic acid, usually added in monomer to reduce reactivity of monomer for stability and easy handling purpose) present in monomer droplet hindered propagation of reaction to form long chain polymer (Niall Behan et al, 2001). The oligomer has PEG at one end and small oligomeric hydrophobic polymer chain which behaves like amphiphiles. Due to

solubility in aqueous phase, oligomers start diffusing in aqueous phase from monomer droplets. As time progress, the concentration of oligomer increases sharply due to which it cross Critical Micellar concentration (CMC) and starts forming micelles (Figure 4.10c). Monomer solubility increases in aqueous phase in presence of surfactant and/or PEG, so monomer start diffusing out of monomer droplets and make micelles richer with monomers. In absence of acidic inhibitors in micellar core, the oligomers start polymerization again by repolymerization process. The diffusion of monomer continues with time and oligomers now turn to long chain polymer. The micelles increase in size with time as polymer chain length increases and lost their micellar properties which turns to NPs (Figure 4.10d).

The fact that NP formation begins concurrently with the oligomer formation rather than high Mw polymer is investigated by N. Behan et al, (2001). Because of amphiphilic nature of oligomer, the particle formation is very uniform and prevents agglomerate formation which otherwise found with unPEGylated PBCA NP. After reduction in monomer availability the polymers in NP start reinitiation-depolymerization-repolymerization process (RDRP) to equilibrate critical degree of polymerization (CDP) of all polymer chains (Ryan B, 1996; Niall Behan et al, 2001). The process of RDRP which is the phenomenon of molecular weight sifting explains why in PBCA NP all polymers have narrow Mw distribution even though very fast polymerization at higher pH (Niall Behan et al, 2001). The RDRP is very important process which consumes unused monomer in NP and reduces toxicity and chance of aggregation of NP. Therefore the PBCA polymer chain describes as a 'truly alive' which reactivated at any time in respond to any change in surrounding environment (Limouzin et al, 2003). This process takes longer time at low pH because of low reaction rate in absence of basic ions. This rate can largely affect by presence of OH ion and can increase by increasing pH of the medium up to five to reduce time needed for reaction completion.

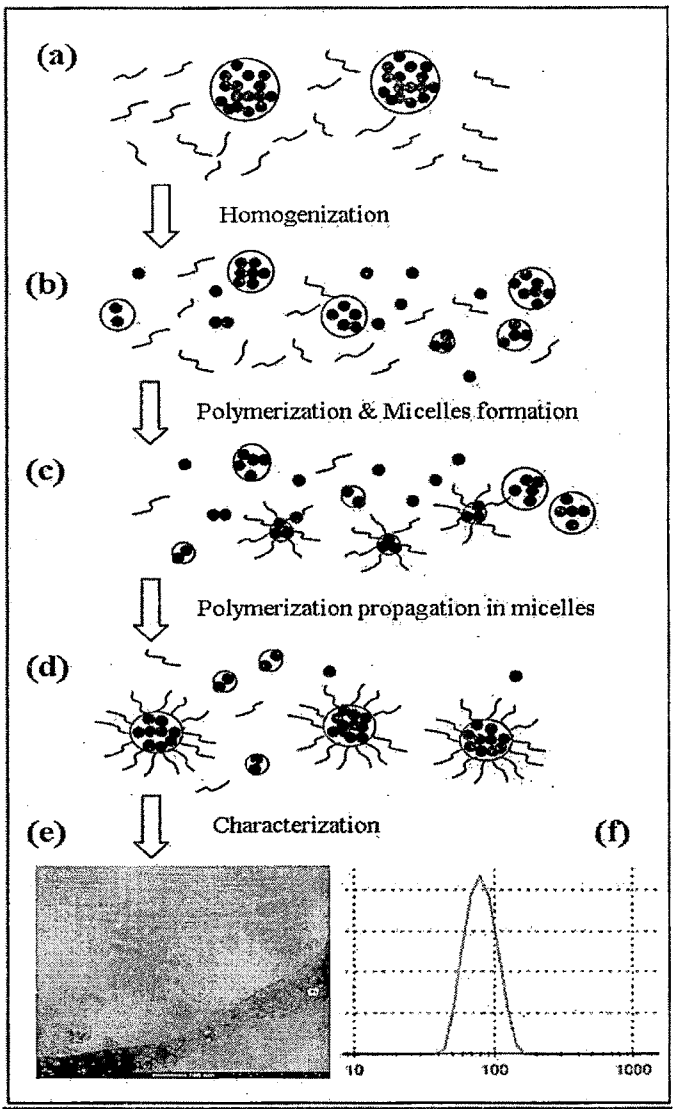

Figure 4.10: PEGylated PBCA NP formation, drug entrapment mechanism (a to d) and characterization by cryoTEM (e) and particle size analysis (f)

Docetaxel is very hydrophobic in nature and soluble in momoner (saturated solubility 7 %). The amount of docetaxel used for NP formulation was 5 % slightly less than saturated solubility. After addition of monomer in to the medium followed by sonication, NP formation starts with micelles formation. Now, because of constant consumption of monomer the content of DTX in monomer exceeded saturation solubility limit and start diffusing from monomer droplets. Due to hydrophobic nature of DTX, it diffuses in

micelles and gets entrapped in micellar core (Figure 4.10d). As time progress, more and more DTX molecules diffuse from monomer droplets and entrapped in inner core of micelles. There is a chance of precipitate formation, but the absence of DTX precipitate and more entrapment of DTX in NP can explain entrapment of DTX in micellar NP. With increase in polymer chain length and size of NPs, the DTX molecule got entrapped permanently in polymer matrix of NPs.

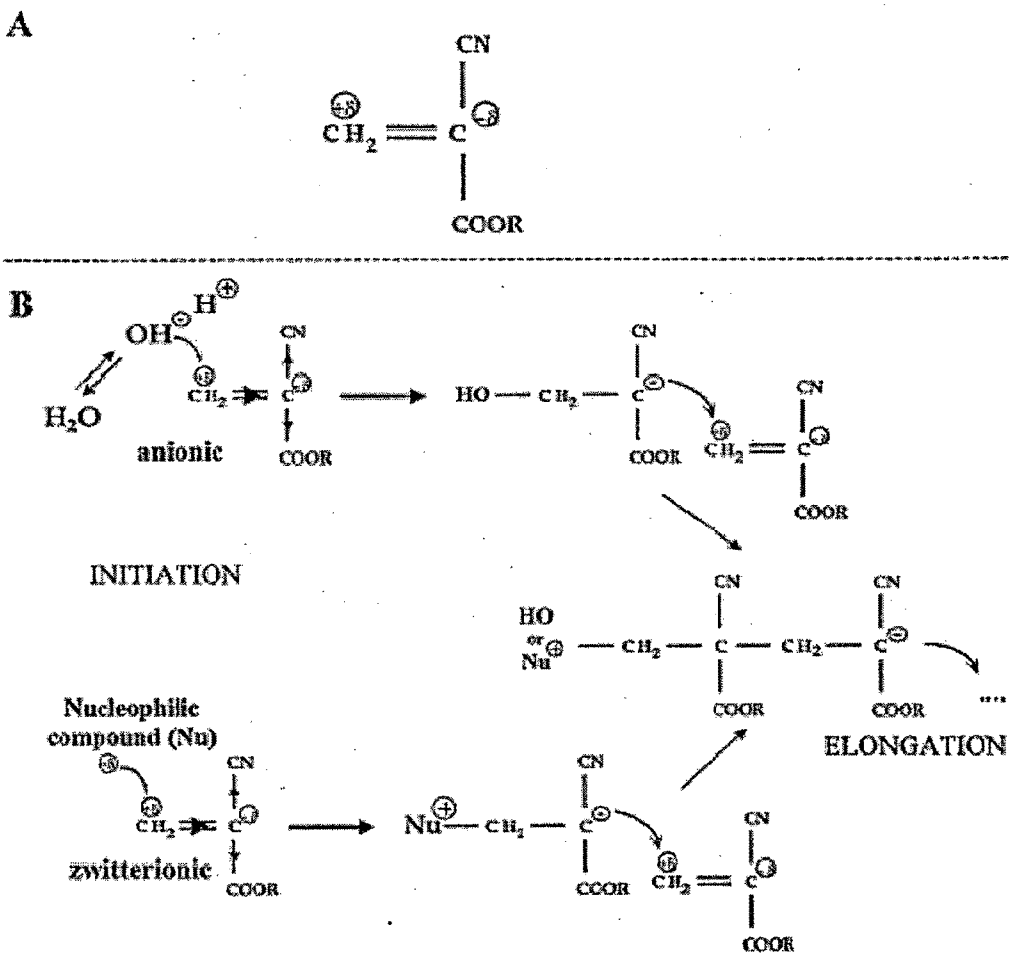

Figure 4.11: A) Alkyl cyanoacrylate molecule B) anionic and nucleophilic initiation of polymerization process of alkyl cyanoacryaltes.

4.3.3.2 Effect of temperature on PBCA NP preparation

With increase in temperature polymerization reaction rate increased sharply and becomes uncontrolled. For NP formation, controlling reaction rate is critically important to get desired size distribution and to prevent aggregation. Polymerization reaction of BCA is very sensitive and susceptible to divert to other undesirable side reaction. In such conditions, reaction at reduced temperature slows down reaction rate, gives preference to PEG as initiator and also avoids other side reactions which are responsible for stoppage of polymer chain reaction and aggregation at later stage.

Effect of temperature on the particle size shown in figure no 4.12. Increase in polymerization temperature from 4-8°C to 20-25°C, It caused particle agglomeration due to increased kinetic energy of the system leading to increased inter-collision of particles (Reddy and Murthy 2004). In addition, efficacy of surfactant to stabilize the particles slowly reduces with increase in temperature thereby causing improper coating of surfactant on NP surface. Further increase in temp up to 45-50 causes extensive agglomeration and visible aggregates in reaction media with in 1 h.

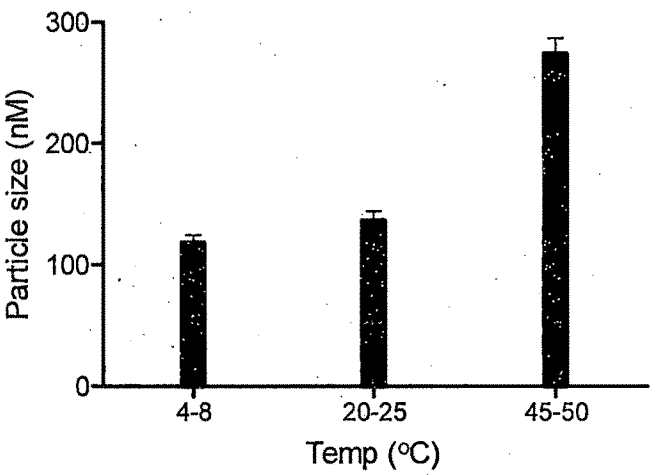

Figure 4.12: Effect of temperature change on particle size of PBCA NP (Data: Mean ±SEM, n = 3)

4.3.3.3 Effect of stirring speed

Stirring speed was found to have influence on particle size (figure 4.13). Because the cyanoacrylate remain in as a droplet form, stirring is necessary to prevent coalescence and reduction in droplet size to give more surface area for diffusion of oligomers and monomer from the surface. At higher speed, the particle size increases slightly with increasing stirring speed (Douglas et al., 1984). This increase is caused by the higher kinetic energy of the system at higher agitation forces. The increased kinetic energy level of the system enables some oligomers, small semisolid particles, and even larger particles to overcome the interfacial energy barrier surrounding the particles, leading the coalescence with other particles (Douglas 1985, Tsukiyama et al., 1974). For the present study the optimized speed was 500 rpm. At low speed there was not enough agitation in the medium resulting in polymerization occurring onto the magnetic stirrer with a resulting increase in particle size and film formation on the surface.

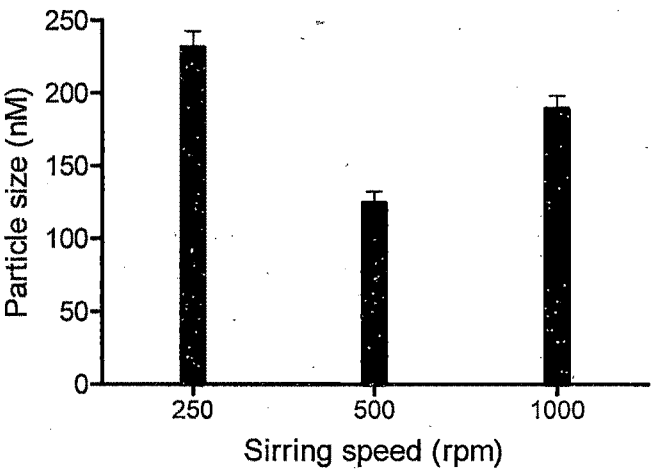

Figure 4.13: Effect of stirring speed on particle size of PBCA NP (Data: Mean ±SEM, n = 3)

4.3.3.4 Effect of surfactant type and concentration

Non-ionic surfactants (poloxamer 188 and 407) provide steric repulsion between the particles causing a reduction in surface tension of the particles resulting in lower particle size (Behan et al., 2001; Huang et al., 2007) which is far better than dextran (figure 4.14). In poloxamers 188 and 407, poloxamer 188 show lower size and more stability.

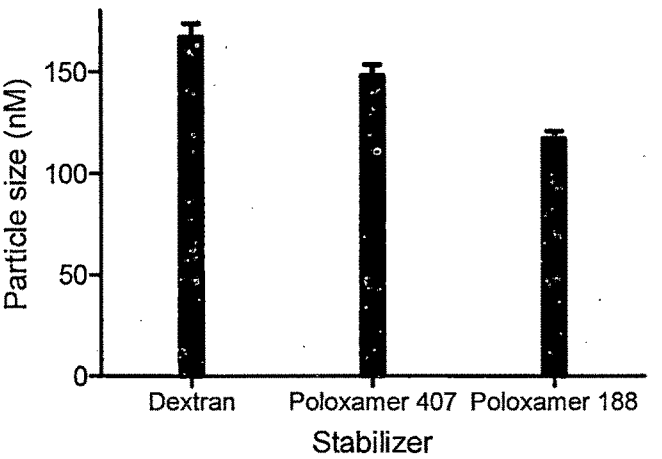

Figure 4.14: Effect of surfactant concentration on particle size and entrapment efficiency of PBCA NPs (Data: Mean ±SEM, n = 3)

The surfactant (poloxamer 188) concentration increased from 0.25% w/v to 1% w/v, the particle size of PBCA NPs decreased (table 4.10). The initial high number of particle nuclei and their small particle size result in a very large total particle surface area. At low stabilizer/surfactant concentration, the amount of stabilizer/surfactant is insufficient to effectively cover the available surface, resulting in an unstable colloidal system. The smaller particles therefore agglomerate until the total particles surface area has decreased to a point such that the amount of poloxamer available is sufficient to produce a stable suspension.

PBCA NPs fabricated with low amount of surfactant show porous and irregular surface (Kreuter 1983; Mitra and Lin 2003) which results in extensive drug loss due to large surface area available for drug to diffuse out from polymer matrix resulting in decreased entrapment efficiency. At increased stabilizer/surfactant concentration, it is possible to stabilize a larger total particle surface area, resulting in the formation of stable particles of a lower size. NPs formed were smooth and nearly spherical in shape with comparatively higher encapsulation efficiency. However, further increase in surfactant concentration beyond 0.5 %w/v showed no further increase in entrapment efficiency. It was interesting to note decrease in zeta potential with increase in surfactant concentration

that may be attributed to shielding of polymer functional group by forming surfactant cloud on the surface of the nanoparticles that shifts the shear plane outwards, resulting in a reduction of the zeta potential (Ballard et al., 1984).

Table 4.12: Effect of surfactant concentration on nanoparticle morphology and drug entrapment (Data: Mean ±SEM, n = 3)

Conc of Poloxamer P188 →	**0.25**	**0.50**	**0.75**	**1.00**
Particle Size (nM)	143 ± 5.34	117 ± 3.48	116 ± 4.75	114 ± 3.98
Zeta Potential (mV)	-21.76 ± 1.81	-17.42 ± 1.36	-11.53 ± 1.43	-8.19 ± 1.71
% Entrap. Efficiency	58.86 ± 3.27	63.82 ± 2.73	62.53 ± 2.43	63.43 ± 3.17

4.3.3.5 Turbidimetric measurements for particle formation

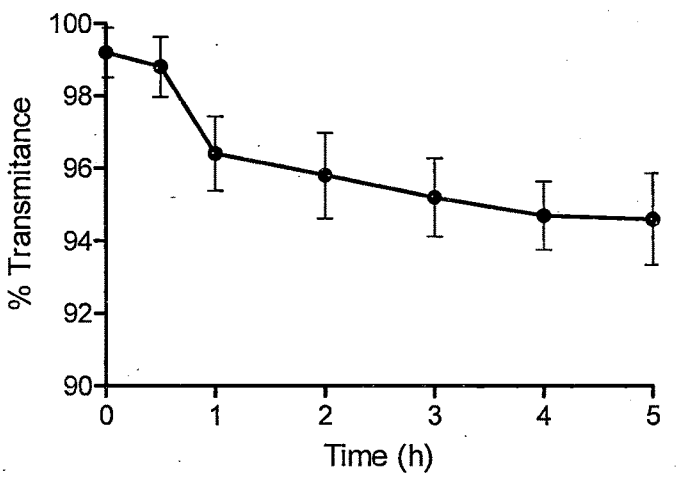

Figure 4.15: Turbidimetric measurement for particle formation with time (Data: Mean ±SEM, n = 3)

An important observation in PBCA polymerization was % transmittance value decreases with increase in polymerization because of conversion of monomer to polymer which increases turbidity. The polymerization is initiated as oligomer formation and propagated in micelles. Because of high degree of compartmentalization of polymerization locus in

presence of surfactant the particle size obtained was very small. The %transmittance values decreases with time indicative of particle formation (Figure 4.15). After four hours there is not much difference in % transmittance values indicating complete monomer conversion into to polymer.

4.3.3.6 Effect of monomer concentration

At low monomer concentrations (≤1% v/v) the amount of monomer molecules available for polymerization being very limited, restricts the size of the NP. However, fast rate of NP formation with more monomer available for reaction with limited amount of initiator tends to change reaction direction to other unfavorable products resulted as stoppage of reaction progress causing aggregation. At high monomer concentration, the primary particles formed undergo further polymerization leading to overall increase in particle size.

Effect of monomer concentration on the drug entrapment efficiency, particle size and zeta potential are depicted in table 4.11. Increase in the monomer concentration in the range between 0.5 % and 2.0%v/v, increased particle size of the NPs. At low monomer concentration, the amount of monomer molecules available for polymerization being very limited restricts the size of the nanoparticles. At high monomer concentration, the primary particles formed undergo saturation with more monomer and further polymerization at this condition leads to overall increase in particle size (Reddy and Murthy, 2003). Such particles would contain polymers of higher molecular weight and could also incorporate more amount of drug. Higher monomer concentration could favor dendritic growth of particles and as a result show more number of functional group on the surface of NP which is evidenced by increase in zeta potential from -12.32 mV to -21.2 mV (Behan et al., 2001; Ballard et al., 1984).

Table 4.13: Effect of monomer concentration on entrapment efficiency, particle size and zeta potential (Data: Mean ±SEM, n = 3)

	Monomer concentration (%v/v)

	0.5	1	1.5	2
Entrap. Efficiency (%)	51.89 ± 3.12	63.13 ± 3.35	68.25 ± 3.54	71.19 ± 2.97
Particle size (nm)	105 ± 4.06	118 ± 4.35	142 ± 5.31	161 ± 6.60
Zeta Potential (mV)	-12.32 ± 2.1	-17.1 ± 1.46	-19.35 ± 1.98	-21.2 ± 2.15

4.3.3.7 Effect of pH on particle size and % drug entrapment

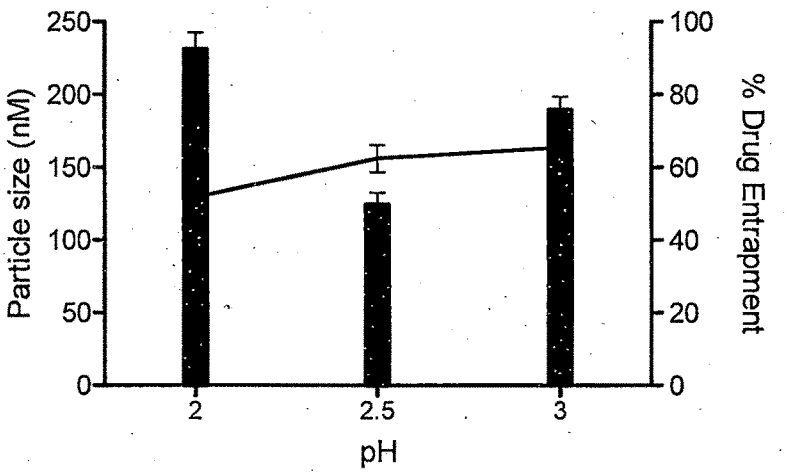

Figure 4.16: Effect of pH on particle size and % drug entrapment in PBCA NP (Data: Mean ±SEM, n = 3)

A pH of 2.5 was found to be optimum for obtaining desire particle size and sufficient entrapment efficiency (Figure 4.16). Polymerization occurs via an anionic mechanism involving initiation by nucleophilic attack on the β-carbon of butyl-2-cyanoacrylate. The resulting carbanion produced reacts with further monomers to form oligomeric chains which nucleate leading to the formation of nanoparticles. The major initiating nucleophile is -OH in case of PBCA NP and nucleophilic attack of amine group in case of PBCA-PEG NP and PBCA-PEG-ZOL NP. pH have dominant influence in both mechanism by change of ionization state of water and amine of PEG. At higher pH, the polymerization rate is too rapid to allow discrete particle formation and leads to direct polymerization of monomer droplets producing an amorphous polymer mass. As pH decreases, the decrease

in reaction rate allows nanoparticles formation to occur. However, if the pH is too low the polymerization period is greatly extended and nanoparticles in this system become swollen with monomer. Coagulation of these semi-fluid particles are not reversible and so produces a polydispersed system of larger particles and larger specific surface area on which molecules of drug can bound. Hence a minimum size and higher loading are observed in the pH profile when polymerization is slow enough to give discrete particles but not so slow as to allow excessive particle coagulation (Douglas et al. 1985).

4.3.3.8 Effect of Docetaxel concentration

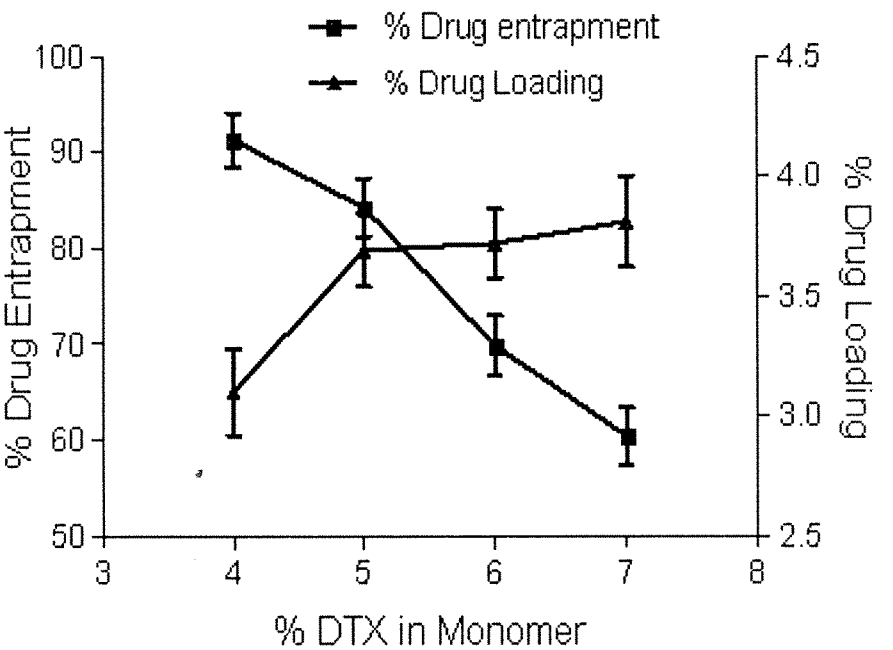

Figure 4.17: Effect of % DTX in monomer on % drug entrapment and % drug loading in PBCA NP (Data: Mean ±SEM, n = 3)

Docetaxel is very hydrophobic in nature and soluble in monomer (saturated solubility 7%). The amount of docetaxel used for NP formulation was 5% slightly less than saturated solubility (figure 4.17). After addition of monomer in to the medium followed by sonication, NP formation starts with micelles formation. Now, because of constant consumption of monomer the content of DTX in monomer exceeded saturation solubility

limit and start diffusing from monomer droplets. Due to hydrophobic nature of DTX, it diffuses in micelles and gets entrapped in micellar core. As time progress, more and more DTX molecules diffuse from monomer droplets and gets entrapped in inner core of micelles. There is a chance of precipitate formation, but the absence of DTX precipitate and more entrapment of DTX in NP can explain entrapment of DTX in micellar NP. With increase in polymer chain length and size of NPs, the DTX molecule got entrapped permanently in polymer matrix of NPs.

4.3.3.9 Effect of PEG on NP formation

The ratio of PEGylation can be control by adjusting feed ratio of PEG to monomer. Ratio of monomer to PEG is very crucial in case of bisamine-PEG for type of block formed. At low PEG mol. concentration (< 50% to monomer conc.), it forms tri-block while at high ((> 50% to monomer conc) it preferably forms diblock copolymer (Peracchia, 1997b). The negative zeta potential of PBCA NP is largely contributed by hydroxyl and may be carbonyl group of polymer present on surface of NPs. With the addition of mPEG, zeta potential start diminishing as a result of PEG replace -OH group and shield other function group on surface of NPs. With triblock formation the zeta potential reduce which gives strong speculation about flower configuration of triblock where PEG graft give nonflexible tight shielding on surface which effectively hides negativity and surface largely exposed with bended PEG chain which is electro-neutral in nature.

The NP formation is directed by micelles formation which is self stabilized system without any need of surfactant. After NP formation, surface of NP will remain covered by grafted PEG which prevent aggregation and stabilized particle in colloidal form. But use of low concentration of surfactant (poloxamer 188, 0.1% w/v)°was found to give good reconstitution ability to formulation after lyophilization. For this reason 0.1% w/v poloxamer 188 was used with PEG. In batches without PEGylation, addition of 0.5% w/v surfactant was found satisfactory. PBCA NP found to have zeta potential well toward negative side (-17.64 mV). With the addition of 20% mol mPEG, negativity of the nanoparticles was reduced to -8.26 mV. However, in case of PBCA-PEG-PBCA NP the zeta potential was found to be still lower (-4.38 mV) (table 4.12, figure 4.18).

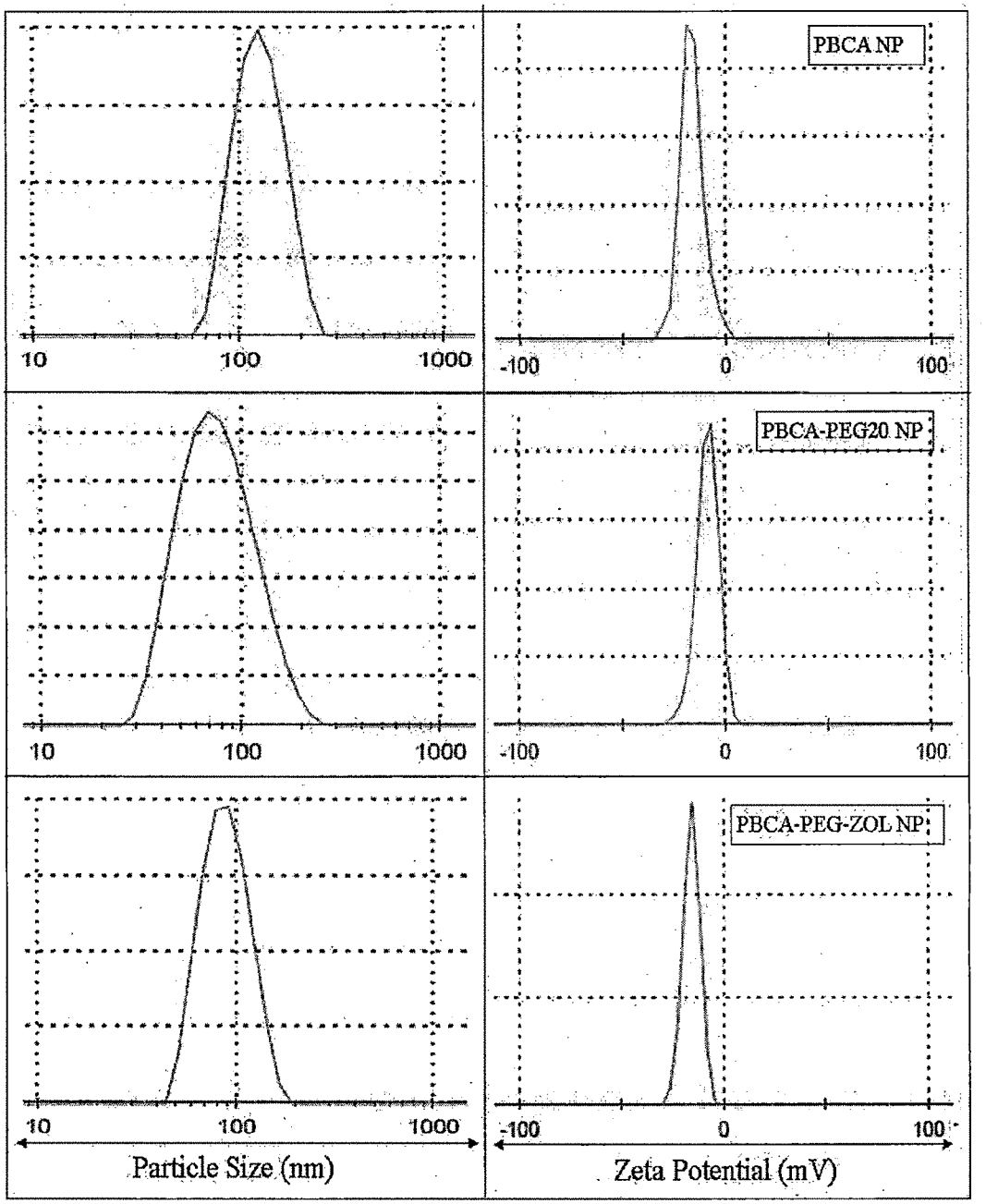

Figure 4.18: Particle size and zeta potential measurement reports of PBCA NP, PBCA-PEG20 NP and PBCA-PEG-ZOL NP (Data: Mean ±SEM, n = 3)

Table 4.14 Characterization of Prepared PBCA NP formulations (Data: Mean ±SEM, n = 3)

Formulation	PEG added (% M)	PEG obtain (% M)	Particle size	Zeta potential	% Drug Entrap ment	% Drug loading	Mw by GPC (Da)
PBCA	0	--	118 ±6.35	-17.64 ±2.21	43.07 ±2.43	2.05 ±0.11	3126
PBCA-PEG5	5	4.76 ±1.54	102 ±7.82	-15.41 ±1.69	51.75 ±3.42	2.46 ±0.13	5948
PBCA-PEG10	10	9.13 ±1.68	89 ±6.81	-13.53 ±1.53	64.58 ±2.86	3.08 ±0.24	6173
PBCA-PEG20	20	17.65± 2.17	81 ±5.63	-8.26 ±1.26	77.38 ±3.20	3.69 ±0.15	5845
PBCA-PEG-PBCA	50	41.52± 4.75	83 ±7.04	-4.38 ±1.08	67.60 ±3.56	3.22 ±0.17	8462
PBCA-PEG-ZOL	20	19.43± 1.37	82± 6.35	-23.51 ±3.37	75.94 ±3.82	3.62 ±0.23	6016

4.2.3.9 6-coumarin loaded PBCA NPs

The particle size and entrapment efficiency for 6-coumarin loaded NPs are tabulated in Table 4.13. 6-coumarin release from PLGA NP was evaluated and show very low burst release at initial 6 h. Hence it can be assumed that the dye does not leach from the NPs during the experimental time frame and therefore the fluorescence seen in the cells is caused by NPs and not by the free dye.

Table 4.15: Particle size and % drug entrapment of 6-coumarin loaded PBCA NP formulations (Data: Mean ±SEM, n = 3)

Formulation	**Particle size (nm)**	**% Drug Entrapment**	**% Burst release in 6 h**
PBCA	121 ± 7.31	52.26 ± 3.24	4.65 ± 0.61
PBCA-PEG5	105 ± 8.25	55.72 ± 4.37	4.83 ± 0.68
PBCA-PEG10	88 ± 8.13	62.81 ± 4.25	5.14 ± 0.62
PBCA-PEG20	83 ± 6.43	74.46 ± 4.21	4.92 ± 0.54
PBCA-PEG-PBCA	84 ± 7.54	69.62 ± 3.96	4.76 ± 0.47
PBCA-PEG-ZOL	81 ± 7.68	76.43 ± 3.89	4.68 ± 0.58

4.3.3.10 In-vitro Drug Release Study

Drug release from biodegradable polymeric nanoparticles depends on the Fickian diffusion through the polymer matrix and on the degradation rate of the polymer. The in-vitro drug release study of lyophilized drug-loaded NPs conducted in phosphate buffer (pH 7.4) containing 10% ethanol and 0.5% v/v tween 80 showed biphasic release (figure 4.19). The initial fast release phase rate is due to the immediate release of drug from the portion of the drug located on and near the surface of the NPs. Thereafter, the release rate decreased as the release rate in this phase is controlled by diffusion rate of drugs across the polymer matrix. In biodegradable matrix systems, the slow release phase depends on the molecular weight and hydrophobicity of the polymer.

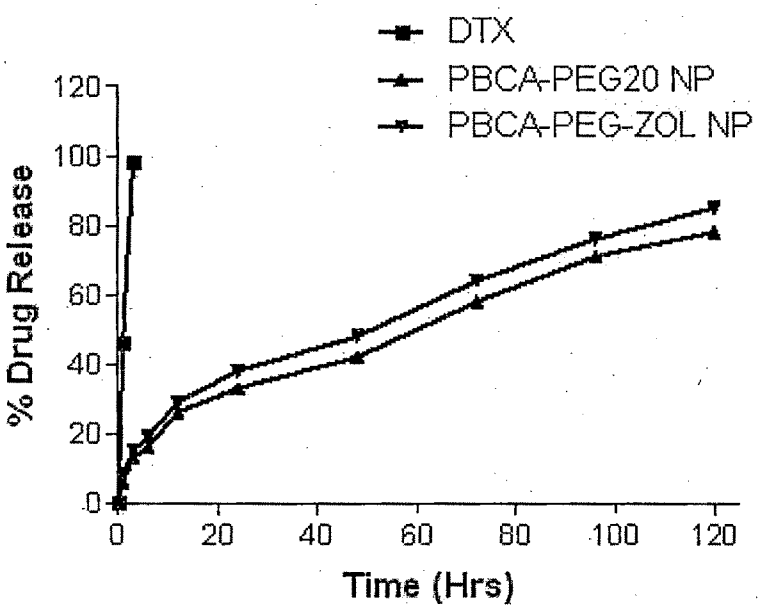

Figure 4.1: In-vitro drug release of DTX and DTX loaded PBCA NP (Data: Mean ±SEM, n = 3)

Report on in vitro study showed that longer hydrophobic alkyl side chains would effectively shield against the hydroxyl ions to attack the ester groups of PBCA polymer and thus decrease the hydrolysis rate of PBCA. In addition presence of larger quantity of

hydrophobic drugs like DTX would contribute to increased hydrophobicity of the polymer matrix resulting in the increased barrier for water and hydroxyl ions to cause degradation of PBCA polymer (Huanga et al, 2007). Therefore, the relative drug release rate decreases with increasing DTX content in particles has been observed. The slow release of DTX also increases speculation of chemical bonding or interaction between groups of DTX with polymer matrix of NPs. This observation also support with earlier report that amine group of drug may also work as an initiator and bonded chemically with PBCA polymer which stop drug release by diffusion (Huanga et al, 2007).

4.3.3.11 FTIR

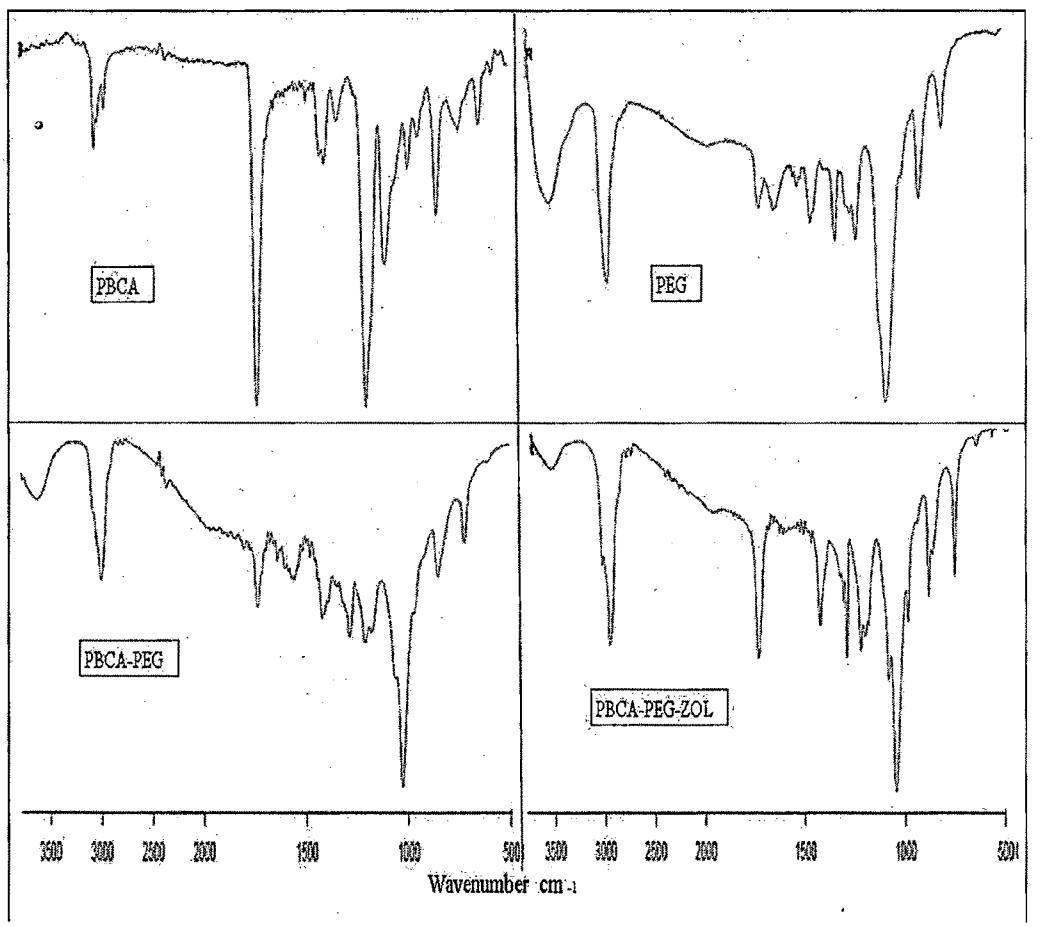

Figure 4.20: FTIR spectra of a) PBCA b) PEG c) PBCA-PEG and d) PBCA-PEG-ZOL

The Fourier transform infrared spectra of the PBCA in Figure 4.20 shows C-H (str) at 2957 cm^{-1} and C-H (def) at 1461 cm^{-1}. The characteristic CΞN (str) of the polymer was observed at 2200 cm^{-1}. The presence of characteristic peaks of PEG and ZOL with PBCA demonstrated successful conjugate formation.

4.3.3.12 NMR spectroscopy

The double bond of vinyl group in the n-butyl cyanoacrylate (monomer) shows peak between 5.0 and 7.0. However there is no peak between 5.0 to 7.0ppm in the NMR spectra of poly(n-butyl cyanoacrylate) i.e. polymer, which indicates the absence of residual monomer and also confirms that complete polymerization of monomer has occurred (figure 4.21). Strong peak at 3.5 ppm demonstrated presence of PEG ($-CH_2-O-CH_2-$). Characteristic peaks from zoledronate also confirm conjugation of PBCA-PEG-ZOL. Peak at 2.5 ppm arise because of solvent (H^2-DMSO) used to dissolve conjugate.

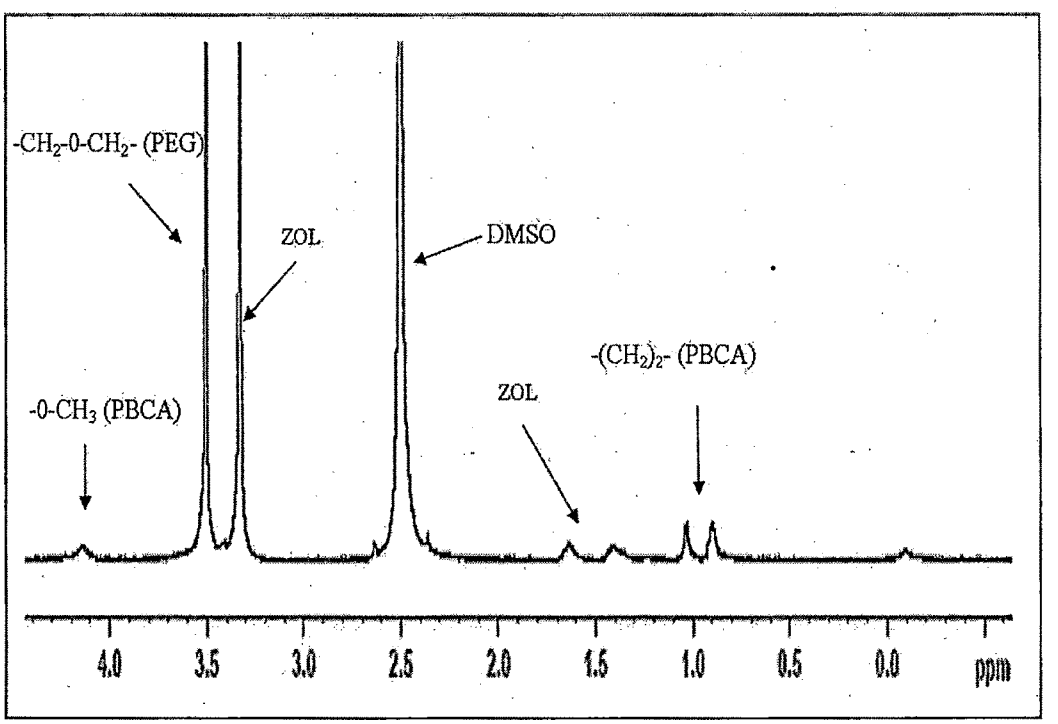

Figure 4.21: H^1 NMR spectra of PBCA-PEG-ZOL conjugate

4.3.3.13 Molecular weight determination

The molecular weight of PBCA nanoparticle was found as below in figure 4.22 by gel permeation chromatography. The molecular weight distribution show good monodispersivity. In case of PEGylated PBCA, average molecular weight is higher in compare to non-PEGylated PBCA and the increase is because of addition of PEG in PBCA chain.

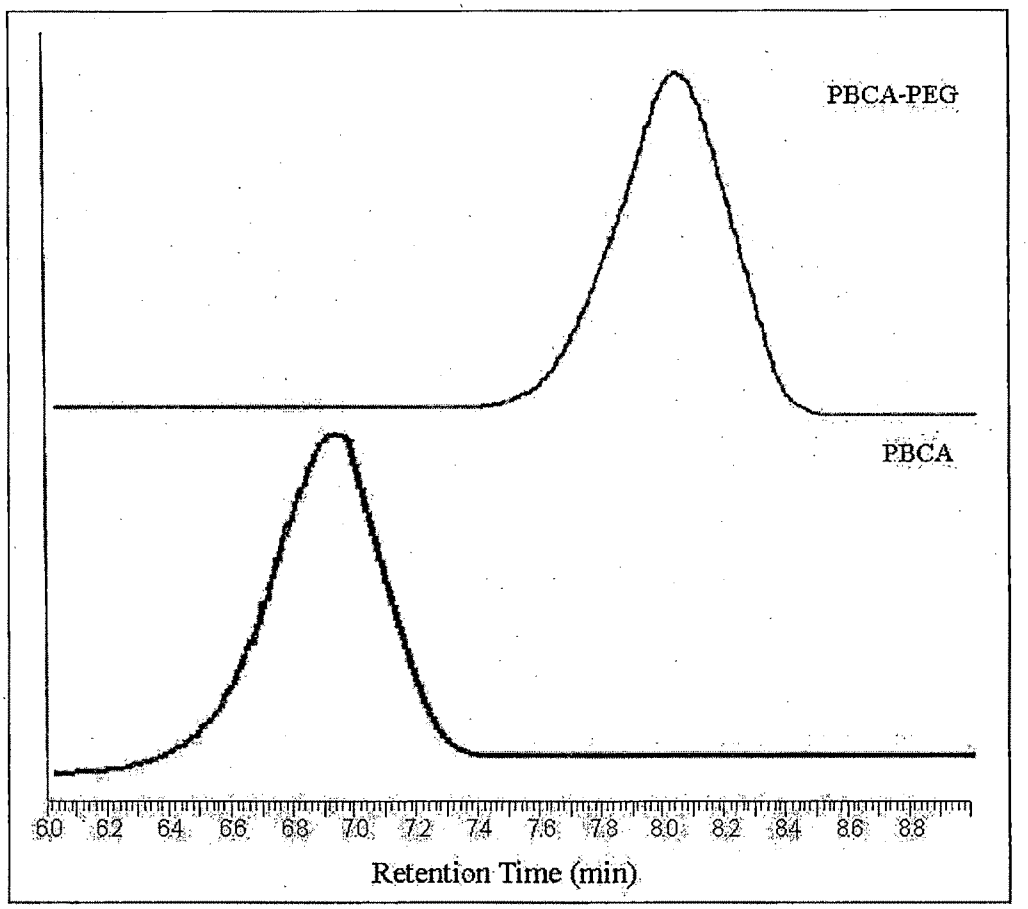

Figure 4.2: Gel Permeations chromatogram of PBCA and PBCA-PEG-ZOL polymer

4.3.3.14 Cryo Transmission Electron Microscopy

The CryoTEM images of PBCA NPs confirmed that the NPs are spherical in shape and in the nanometric range. PBCA NP size determined from zeta sizer was found similar with

the size shown in CryoTEM image. Figure 4.23 illustrates Cryo TEM image of DTX loaded PBCA NPs.

a)

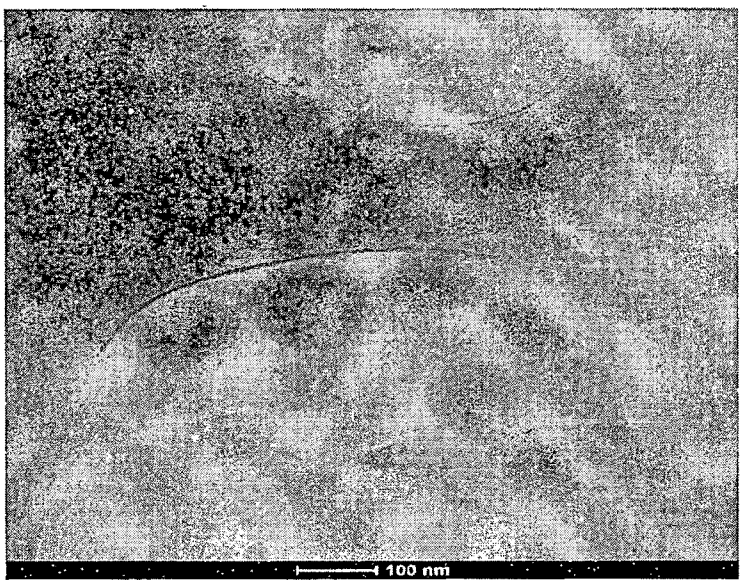

b)

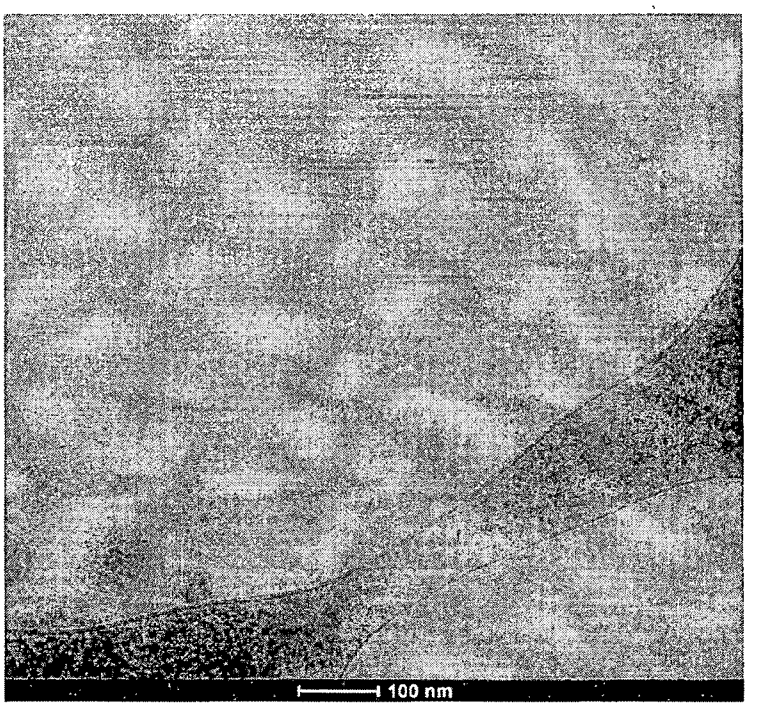

Figure 4.23: TEM image of a) PBCA NPs, b) PBCA-PEG-ZOL NP

4.3.3.15 Differential scanning calorimetry

DSC thermograms demonstrated that only pure DTX had an endothermic peak of melting at 210°C (aprox) whereas control or drug-loaded NPs had no such peak in the range 150-250 °C (Figure 4.24). The results thus indicate that DTX encapsulated in NPs is in the amorphous or disordered-crystalline phase of a molecular dispersion or in the solid-state solubilized form in the polymer matrix of NPs after fabrication (Mu and Feng, 2002, Esmaeili et al., 2008).

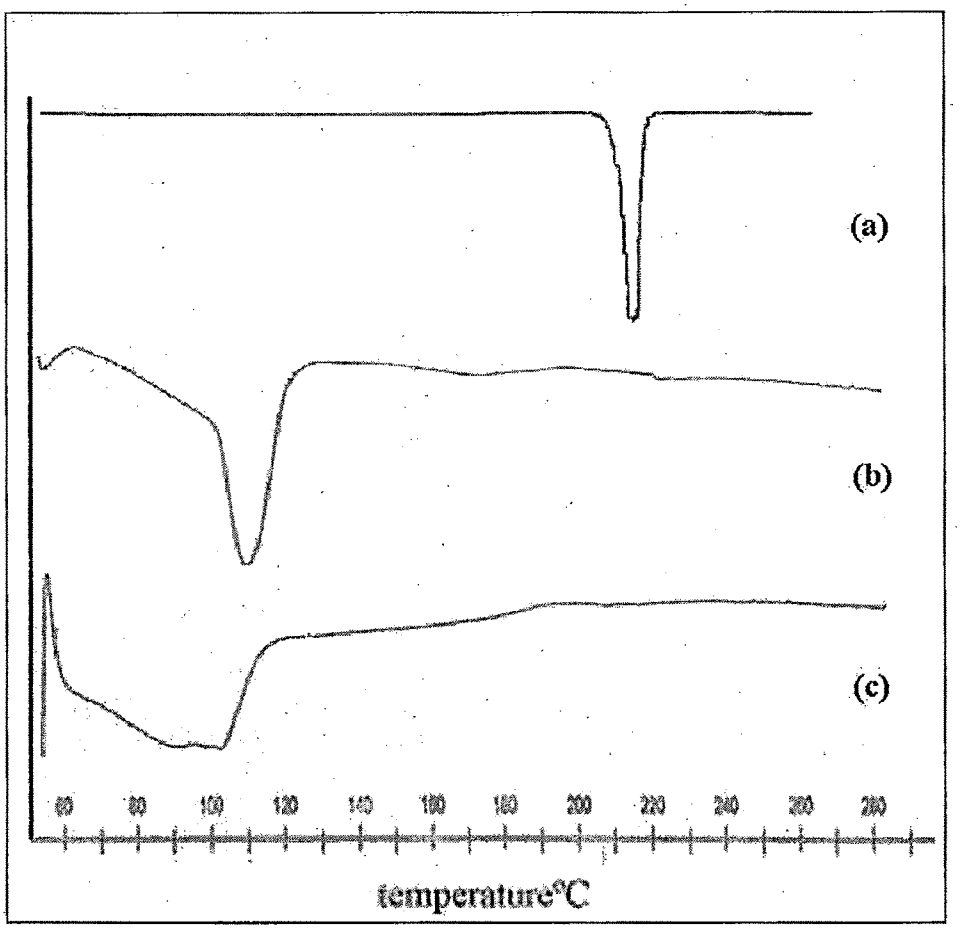

Figure 4.24: DSC study of (a) DTX, (b) PBCA-PEG-ZOL, and (c) DTX loaded PBCA-PEG-ZOL NP

4.3.3.16 Residual poloxamer in formulation

After washing step the residual amount of poloxamer P188 was estimated in each PBCA formulation. Result found that nonPEGylated formulation PLGA NP having highest residual poloxamer P188 concentration (table 4.14). It can be conclude that poloxamer P188 bound on the surface of PBCA NP by hudrophobic interaction or/and by covalent attachment. After attachment of PEG the poloxamer adsorption was found reduced. The estimated residual amount is shown in table 4.6 in final lyophilized formulation.

Table 4.16: Amount of residual poloxamer P188 in PBCA NP formulations (Data: Mean ±SEM, n = 3)

Formulation	Poloxamer P188 added (% w/v)	Residual Poloxamer P188 added (% w/v)
PBCA NP	0.5	0.36 ± 0.043
PBCA-PEG5 NP	0.1	0.32 ± 0.036
PBCA-PEG10 NP	0.1	0.18 ± 0.027
PBCA-PEG20 NP	0.1	0.17 ± 0.022
PBCA-PEG-PBCA NP	0.1	0.16 ± 0.041
PBCA-PEG-ZOL NP	0.1	0.19 ± 0.029

4.3.3.17 Salt and serum induced aggregation study

Comparative evaluation of aggregation resistance property of PEGylated and non-PEGylated NPs was performed using salt induced aggregation and serum induced aggregation technique. Result showed that out of all formulation PBCA-PEG20 NPs and PBCA-PEG-PBCA NPs displayed exceptionally high resistance to aggregation (Fig. 4.25a and 4.25b). Results of serum induced aggregation showed no significant increase in particle size with PBCA-PEG20 NPs and PBCA-PEG-PBCA NPs, PBCA-PEG10 NPs showed slight increase with time while PBCA-PEG5 NPs and PBCA NPs showed dramatic increase in particle size with time (Fig. 4.25c).

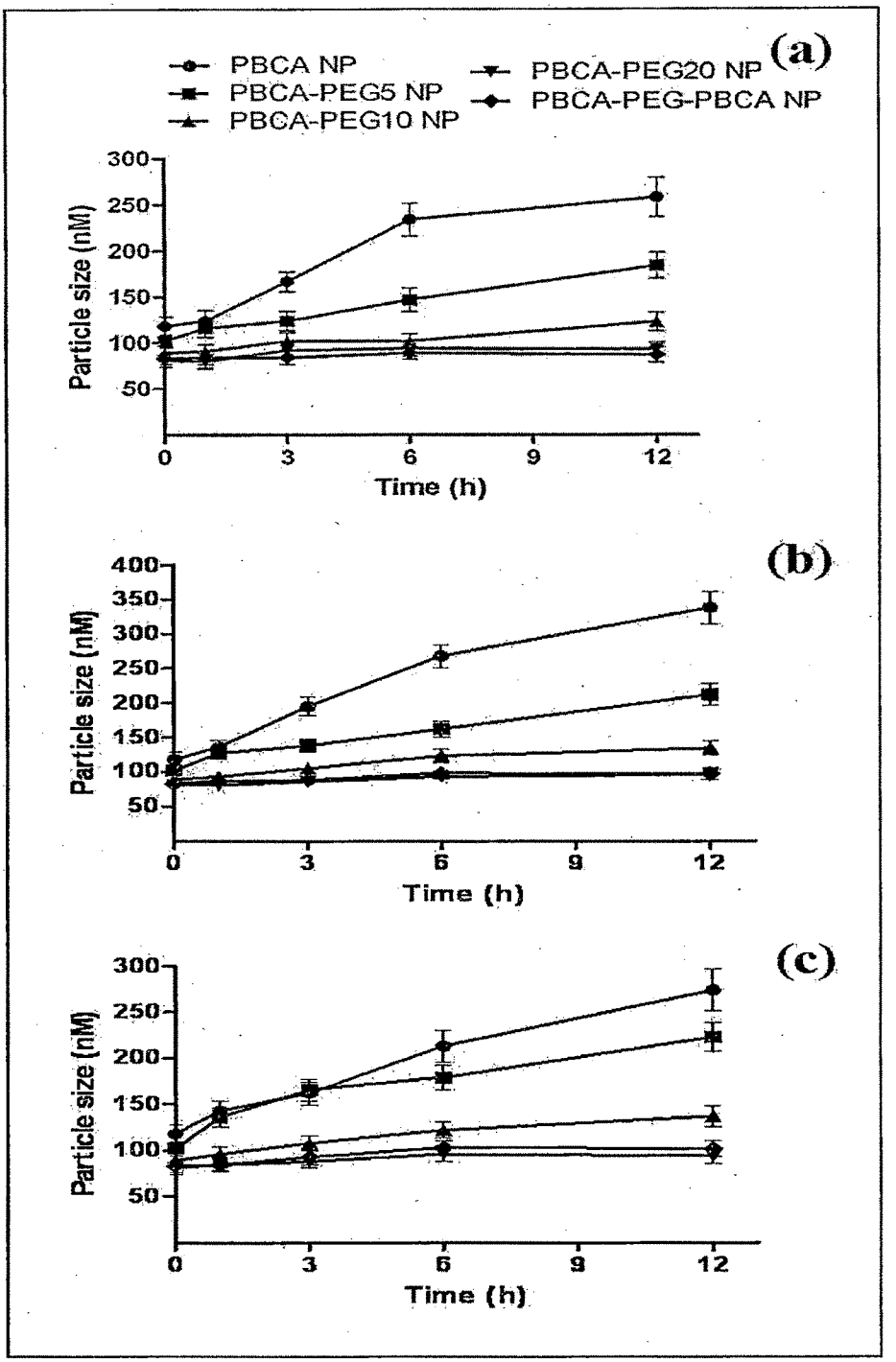

Figure 4.25: Colloidal stability study using salt induced aggregation using (a): Na_2SO_4 and (b): $CaCl_2$. (c): Serum stability study of NP formulations in phosphate buffer saline (pH 7.4) containing 1% FBS. (Data: Mean ±SEM, n = 3)

NPs with PEG grafting have very slight increase in particle size while non-PEGylated NPs show drastic rise in particle size which shows liability of NPs for aggregation. The process of phagocytosis initiated with adsorption of serum protein which enhance recognition by macrophage cells. It is well established that phagocytosis is a cellular phenomenon and initiated by the attachment of the foreign particles to the surface receptors of the phagocytic cells (Pratten and Lioyd, 1986). And this attachment can be facilitated by the absorption of plasma proteins (opsonins) to the particle surface (Moghimi and Patel, 1998; Blunk et al, 1993). Muller and co-workers illustrated that PLLg-PEG coated PLGA microspheres showed low protein adsorption compared to uncoated PLGA microspheres (Muller et al, 2003). Hence adsorption of protein is an important parameter to evaluate *in vitro* and to predict stability of NPs *in vivo*. After protein adsorption, size of NPs increase and it become highly prone to aggregation in serum containing media. The adsorption of serum protein was assisted by electrostatic and hydrophobic interaction of protein with NPs surface. With protein adsorption, size of NP starts increasing and also caused aggregation. NPs with PEG graft at surface provide protein repellent property and offer no hydrophobic or electrostatic interaction for protein thus colloidal solution remain stable for long time.

4.3.3.18 In vitro bone binding affinity assay

In vitro bone affinity study was carried out to evaluate bone binding property of zoledronic acid before and after conjugation with PBCA NP. Zoledronic acid found to have strong bone binding affinity. Figure 4.26 demonstrated that more than 95% zoledronic acid was found with bone in bound form within 6 h. The affinity of zoledronic acid conjugated with PBCA NP also found only slight difference to free zoledronic acid. After 6 h zoledronic acid conjugated PBCA NP shown more than 90% bone binding affinity.

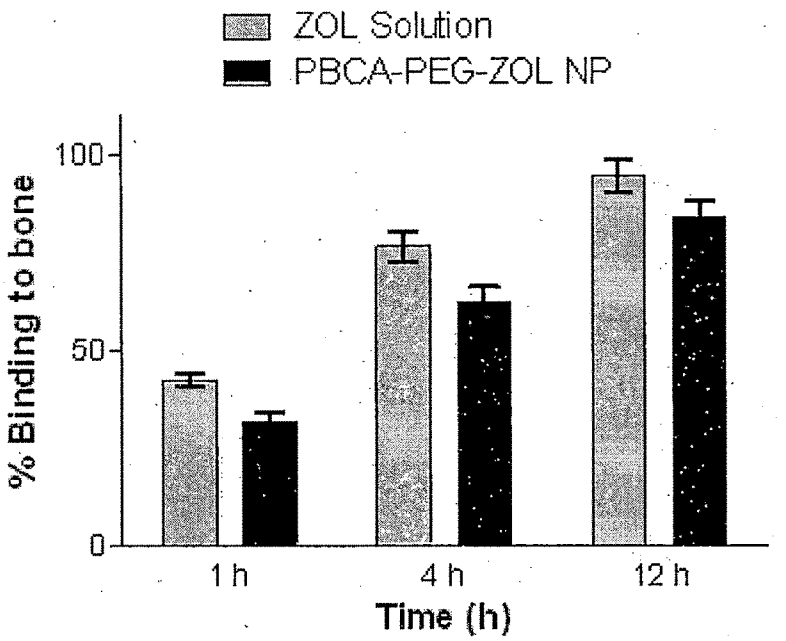

Figure 4.26: In vitro bone binding affinity assay of ZOL solution and PBCA-PEG-ZOL NP (Data: Mean ±SEM, n = 3)

4.3.3.19 Selection of cryo-protectants for lyophilization

Trehalose was found to be the most effective cryo-protectant for lyophilization of the PBCA NPs at a NP: Sugar ratio of 1:5. Sucrose did not have any protective effect on particles size of NPs at any concentration tested in the present study and form aggregate during reconstitution. The lyophilized particle prepared using mannitol were found to be re-dispersed easily but there was a great increase in size as compared to those prepared with trehalose. Hence, trehalose is selected as an effective cry-oprotectant in the present study. The results are tabulated in table 4.15.

The different batches of the NPs were subjected to visual examination and each batch of NPs was analyzed for particle size, drug content and reconstitution property. Aggregation and drug leaching is a common problem in case of nanoparticulate dispersions as observed from the results. Hence, the dispersions are lyophilized in presence of cryoprotectants to maintain the stability of the dispersions on freeze drying.

Table 4.17: Effect of different cryo-protectant on particle size and reconstitution property (Data: Mean ±SEM, n = 3)

Cryo-protectant	NPs: CP	Particle size (nm)		Reconstitution time (sec)	Redispersibility
		Before	After		
None	1:0	118± 6.35	--	--	lump formation
Sucrose	1:1		--	--	lump formation
	1:3		221 ± 16.3	190	few aggregates
	1:5		189 ±12.8	160	clear solution
Mannitol	1:1		209 ± 10.5	190	few aggregates
	1:3		182 ± 11.0	120	clear solution
	1:5		163 ± 7.6	90	clear solution
Trehalose	1:1		174 ± 7.2	90	few aggregates
	1:3		136 ± 6.7	60	clear solution
	1:5		127 ± 5.1	40	clear solution

4.3.4 Stability studies

The stability studies were carried out according to ICH guidelines for drug substances intended for storage in a refrigerator. The long term stability study of lyophilized NPs was carried out at 5°Ç ± 3°C for six months. The nanoparticles short term stability was conducted for three months at 25 ± 2°C/60 ± 5% RH. Sampling was done at 15 days, 1, 2, 3 and 6 months. The stability profiles are shown in tables 4.16.

It can be observed that when stored at 5°C ± 3°C, NPs are stable up to a period of six months with no significant change in either particle size, zeta potential or the drug content. The short term studies also indicate that nanoparticle formulation when stored at 25 ± 2°C/60 ± 5% RH are also stable with no significant change in drug content. All the samples stored at 5°C ± 3°C and 25 ± 2°C/60 ± 5% RH were redispersed easily within 2 minutes.

Hence, it can be concluded that the NPs should be stored at 5°C ± 3°C for maximum stability and a long term stability study (1 - 2 years) is necessary for determining the optimum storage conditions for the lyophilized NPs.

Table 4.18: Stability data for DTX loaded PBCA based NP formulations (Data: Mean ±SEM, n = 3)

Time	Particle size (nm) ± SEM	Zeta potential (mV) ± SEM	Drug content (%) ± SEM	Reconstitution time (sec)	Reconstitution property
Initial	82 ± 6.4	-23.51 ±3.37	100	40	clear solution
5°C ± 3°C					
0.5	84 ± 5.6	-24.63 ± 2.26	99.4 ± 0.76	40	clear solution
1	84 ± 5.6	-23.15 ± 2.31	98.5 ± 1.62	50	clear solution
2	89 ± 6.4	-24.77 ± 1.78	97.1 ± 1.63	60	clear solution
3	93 ± 6.0	-23.34 ± 2.07	96.8 ± 2.15	70	clear solution
6	98 ± 7.1	-23.28 ± 1.56	95.4 ± 2.39	70	clear solution
25 ± 2°C/60 ± 5% RH					
0.5	85 ± 4.2	-23.62 ± 1.65	98.8 ± 1.34	50	clear solution
1	89 ± 6.1	-22.96 ± 2.11	98.1 ± 1.45	60	clear solution
2	93 ± 5.8	-23.31± 2.18	97.3 ± 1.36	70	clear solution
3	105 ± 7.3	-22.18 ± 1.97	95.6 ± 2.28	90	clear solution

4.3.5 Conclusion

We can conclude that novel PBCA fabrication and PEGylation method gives desire size in nanoscale as well as conjugate PEG effectively in single step polymerization and nanoparticle formation. Prepared method also gives good entrapment with DTX because of emulsion micelles formation. Characterization of NP as PEGylation result also found

satisfactory and fould suitable for parenteral administration. PEGylation and ZOL conjugation of PBCA NPs can be done effectively without significant change in morphology of the NPs other than particle size and zeta potential. DTX entrapped PBCA NP formulations demonstrated sustained release effect. PBCA based NP formulations found good stability while storage condition was refrigerated (2 - 8°C) for 6 months.

4.4 Reference

1. Wu X.S., Synthesis and properties of biodegradable lactic/glycolic acid polymers, in: Wise, et al., (Eds.), Encyclopedic handbook of biomaterials and bioengineering, Marcel Dekker, New York, 1995, pp. 1015–1054.
2. Lu J.M., Wang X., C. Marin-Muller, H. Wang, P.H. Lin, Q. Yao, C. Chen, Current advances in research and clinical applications of PLGA-based nanotechnology, Expert Rev. Mol. Diagn. 9 (2009) 325–341.
3. U. Bilati, E. Allemann, E. Doelker, Development of a nanoprecipitation method intended for the entrapment of hydrophilic drugs into nanoparticles, Eur. J. Pharm. Sci. 24 (2005) 67–75.
4. P.A. Rivera, M.C. Martinez-Oharriz, M. Rubio, J.M. Irache, S. Espuelas, Fluconazole encapsulation in PLGA microspheres by spray-drying, J. Microencapsul. 21 (2004) 203–211.
5. F.Y. Cheng, S.P. Wang, C.H. Su, T.L. Tsai, P.C. Wu, D.B. Shieh, J.H. Chen, P.C. Hsieh, C.S. Yeh, Stabilizer-free poly (lactide-co-glycolide) nanoparticles for multimodal biomedical probes, Biomaterials 29 (2008) 2104–2112.
6. S. Parveen, S.K. Sahoo, Polymeric nanoparticles for cancer therapy, J. Drug Target. 16 (2008) 108–123.
7. S.K. Sahoo, J. Panyam, S. Prabha, V. Labhasetwar, Residual polyvinyl alcohol associated with poly (D, L-lactide-co-glycolide) nanoparticles affects their physical properties and cellular uptake, J. Control. Release 82 (2002) 105–114.
8. J. Panyam, W.Z. Zhou, S. Prabha, S.K. Sahoo, V. Labhasetwar, Rapid endolysosomal escape of poly (DL-lactide-co-glycolide) nanoparticles: implications for drug and gene delivery, FASEB J. 16 (2002) 1217–1226.
9. F. Alexis, E. Pridgen, L.K. Molnar, O.C. Farokhzad, Factors affecting the clearance and biodistribution of polymeric nanoparticles, Mol. Pharm. 5 (2008) 505–515.
10. R. Gref, Y. Minamitake, M.T. Peracchia, V. Trubetskoy, V. Torchilin, R. Langer, Biodegradable long-circulating polymeric nanospheres, Science 263 (1994) 1600–1603.
11. D.E. Owens, N.A. Peppas, Opsonization, biodistribution, and pharmacokinetics of polymeric nanoparticles, Int. J. Pharm. 307 (2006) 93–102.

12. J. Khandare, T. Minko, Polymer–drug conjugates: Progress in polymeric prodrugs, Prog. Polym. Sci. 31 (2006) 359–397.
13. S. Alila, A.M. Ferraria, A.M. Botelho do Rego, S. Boufi, Controlled surface modification of cellulose fibers by amino derivatives using N,N'-carbonyldiimidazole as activator, Carbohydr. Polym. 77 (3) (2009) 553–562.
14. H. Fessi, F. Puisieux, J.Ph. Devissaguet, N. Ammoury, S. Benita, Nanocapsule by interfacial polymer deposition following solvent displacement, Int. J. Pharm. 55 (1) (1989) R1–R4.
15. Peracchia MT, Vauthier C, Passirani C, Couvreur P, Labarre D. Complement consumption by poly(ethylene glycol) in different conformations chemically coupled to poly(isobutyl 2-cyanoacrylate) nanoparticles. Life Sci. 1997;61(7):749-761.
16. International Conference on Harmonisation, www.ich.org/products/guidelines.
17. Davis JT, Rideal EK. Interfacial phenomena. J. Electrochem. Soc. 109 (7) (1962)175C-175C.
18. Quintanar-Guerrero D, Allemann E, Fessi H, Doelker E. Preparation techniques and mechanisms of formation of biodegradable nanoparticles from performed polymers. Drug Dev. Ind. Pharm. 24 (12) (1998) 1113–1128.
19. Derakhshandeh K, Erfan M, Dadashzadeh S. Encapsulation of 9-nitrocamptothecin, a novel anticancer drug, in biodegradable nanoparticles: Factorial design, characterization and release kinetics. European J. of Pharm. and Biopharm 66 (2007) 34–41.
20. Govender T, Riley T, Ehtezazi T, Garnett MC, Stolnik S, Illum L, Davis SS. Defining the drug incorporation properties of PLA–PEG nanoparticles. Int. J. Pharm. 199 (2000) 95–110.
21. Chorny M, Fishbein I, Danenberg HD, Golomb G. Lipophilic drug loaded nanospheres prepared by nanoprecipitation: effect of formulation variables on size, drug recovery and release kinetics. J. of Control Rel 83 (2002) 389–400.
22. Song X, Zhao Y, Hou S, Xu F, Zhao R, He J, Cai Z, Li Y, Chen Q. Dual agents loaded PLGA nanoparticles: systematic study of particle size and drug entrapment efficiency. European J. of Pharm Biopharm 69 (2008a) 445-453.

23. Song X, Zhao Y, Wu W, Bi Y, Cai Z, Chen Q, Li Y, Hou S. PLGA nanoparticles simultaneously loaded with vincristine sulfate and verapamil hydrochloride: Systematic study of particle size and drug entrapment efficiency. Int. J. Pharm 350 (2008b) 320–329.
24. Budhian A, Siegel SJ, Winey KL. Haolperidol loaded PLGA nanoparticles: systematic study of particle size and drug content. Int. J. of Pharm 336 (2007) 367-375.
25. Behan N, Birkinshaw C, Clarke N. Poly n- butyl cyanoacrylate nanoparticles: a mechanistic study of polymerization and particle formation. Biomaterials 22 (2001) 1335-1344.
26. Huang CY, Chen CM, Lee YD. Synthesis of high loading and encapsulation efficient paclitaxel-loaded poly(n-butyl cyanoacrylate) nanoparticles via miniemulsion. Int. J. of Pharm. 338 (2007) 267–275.
27. Boury F, Ivanova T, Panaitov I, Proust JE, Bois A, Richou J. Dynamic properties of poly(DL-lactide) and polyvinly alcohol monolayers at the air/water and dichloromethane/water interfaces. J Colloid Interf. Sci. 169 (1995) 380-392.
28. Rodriguez SG, Allemann E, Fessi H, Doelkar E. Physicochemical parameters associated with nanoparticle formation in the saltingout, emulsification-diffussion and nanoprecipitation methods. Pharm. Res. 21 (2004) 1428-1439.
29. Rizkalla N, Range C, Lacasse FX, Hildgen P. Effect of various formulation parameters on the properties of polymeric nanoparticles prepared by multiple emulsion method. J. Microencap 23(1): (2006) 39–57.
30. Ballard M, Napper D, Gilbert R. Kinetics of emulsion polymerization of methyl methacylate. J of Polymer Sci: Polymer Chemistry edition. 22 (1984) 3225-3253.
31. Hyvonen S, Peltonen L, Karjalainen M, Hirvonen J. Effect of nanoprecipitation on the physicochemical properties of low molecular weight poly(l-lactic acid) nanoparticles loaded with salbutamol sulphate and beclomethasone dipropionate. Int. J of Pharm 295 (2005) 269–281.
32. Vandervoort J, Ludwig A. Biocompatible stabilizers in the preparation of PLGA nanoparticles: a factorial design study. Int. J. Pharm 238 (2002) 77–92.

33. Franks, F. Freeze-drying of bioproducts: putting principles into practice. Eur. J. Pharm. Biopharm. 45(1998) 221–229.
34. Saez A, Guzman M, Molpeceres J, Aberturas MR. Freeze drying of polycaprolactone and poly(D,L-lactic-glycolic) nanoparticles induce minor particle size changes affecting the oral pharmacokinetics of loaded drugs. Eur. J. Pharm. Biopharm. 50 (2000) 379–387.
35. Sameti M, Bohr G, Ravi Kumar MNV, Kneuer C, Bakowsky U, Nacken M, Schmidt H, Lehr CM. Stabilisation by freeze-drying of cationically modified silica nanoparticles for gene delivery. Int. J. Pharm. 266 (2003) 51–60.
36. Yu L, Mishra DS, Rigsbee DR. Determination of the glass properties of D-mannitol using sorbitol as an impurity. J. Pharm. Sci. 87 (1998) 774–777.
37. Konan YN, Gurny R, Konan YN, Gurny R. Preparation and characterization of sterile and freeze-dried sub-200nm nanoparticles. Int J Pharm 233 (2002) 239–352.
38. Mu L, Feng SS. PLGA/TPGS nanoparticles for controlled release of paclitaxel: effects of the emulsifier and the drug loading ratio. Pharm Res 20(11) (2003) 1864–1872.
39. Magenheim B, Levy MY, Benita S. A new in vitro technique for evaluation of drug release profile from colloidal carriers-ultrafiltration technique at low pressure. Int. J. Pharm. 94 (1993) 115–123.
40. Esmaeili et al., PLGA nanoparticles of different surface properties: Preparation and evaluation of their body distribution, Int. J. Pharm 349 (2008) 249–255.
41. Woods. Cyanoacrylates. In: J.C. Salamone (Eds.), Polymeric materials encyclopedia, Vol. 2. CRC Press Inc, New York, (1996) pp, 1632–1637.
42. Kreuter J, Petrov VE, Kharkevich DA, Alyautdin RN. Influence of the type of surfactant on the analgesic effects induced by the peptide dalargin after its delivery across the blood–brain barrier using surfactant-coated nanoparticles. J. Control. Release. 49 (1997) 81–87.
43. Müller RH, Lherm C, Herbort J, Blunk T, Couvreur P. Alkylcyanoacrylate drug carriers: I. Physicochemical characterization of nanoparticles with different alkyl chain length. Int J Pharm 84 (1992) 1–11.

44. Müller RH, Lherm C, Herbort J, Couvreur P. In vitro model for the degradation of alkylcyanoacrylate nanoparticles. Biomaterials 11 (1990) 590–595.

45. Lherm C, Müller RH, Puisieux F, Couvreur P. Alkylcyanoacrylate drug carriers: II. Cytotoxicity of cyanoacrylate nanoparticles with different alkyl chain length. Int J Pharm 84 (1992) 13–22.

46. Kante B, Couvreur P, Dubois-Krack G, De Meester C, Guiot P, Roland M, Mercier M, Speiser P. Toxicity of polyalkylcyanoacrylate nanoparticles I: Free nanoparticles. J Pharm Sci 71 (1982) 786-90.

47. Pereverzeva E, Treschalin I, Bodyagin D, Maksimenko O, Kreuter J, Gelperina S. Intravenous tolerance of a nanoparticle-based formulation of doxorubicin in healthy rats. Toxicol. Lett. 2008;178(1): 9–19.

48. Gelperina SE, Khalansky AS, Skidan IN, Smirnova ZS, Bobruskin AI, Severin SE, Turowski B, Zanella FE, Kreuter J. Toxicological studies of doxorubicin bound to polysorbate 80-coated poly(butyl cyanoacrylate) nanoparticles in healthy rats and rats with intracranial glioblastoma. Toxicol. Lett. 2002;126(2):131–141.

49. Pereverzeva E, Treschalin I, Bodyagin D, Maksimenko O, Langer K, Dreis S, Asmussen B, Kreuter J, Gelperina S. Influence of the formulation on the tolerance profile of nanoparticle-bound doxorubicin in healthy rats: focus on cardio- and testicular toxicity. Int. J. Pharm. 2007;337(1-2):346–356.

50. Zhou Q, Sun X, Zeng L, Liu J, Zhang Z. A randomized multicenter phase II clinical trial of mitoxantrone-loaded nanoparticles in the treatment of 108 patients with unresected hepatocellular carcinoma. Nanomedicine. 2009;5(4):419–423.

51. Vauthier C, Dubernet C, Chauvierre C, Brigger I, Couvreur P. Drug delivery to resistant tumors: the potential of poly(alkyl cyanoacrylate) nanoparticles. J. Controlled Release. 2003;93(2):151–160.

52. Couvreur P, Kante B, Roland M, Guiot P, Baudhuin P, Speiser P. Polycyanoacrylate nanocapsules as potential lysosomotropic carriers: preparation, morphological and sorptive properties. J. Pharm. Pharmacol. 1979;31(5):331–332.

53. Peracchia MT, Vauthier C, Puisieux F, Couvreur P. Development of sterically stabilized poly(isobutyl 2-cyanoacrylate) nanoparticles by chemical coupling of poly(ethylene glycol). J. Biomed. Mater. Res., Part A. 1997(a);34(3):317-326.

54. Peracchia MT, Vauthier C, Passirani C, Couvreur P, Labarre D. Complement consumption by poly(ethylene glycol) in different conformations chemically coupled to poly(isobutyl 2-cyanoacrylate) nanoparticles. Life Sci. 1997(b);61(7):749-761.

55. De Juan BS, Briesen HV, Gelperina SE, Kreuter J. Cytotoxicity of doxorubicin bound to poly(butyl cyanoacrylate) nanoparticles in rat glioma cell lines using different assays. J. Drug Targeting. 2006;14(9):614–622.

56. Mitra A, Lin S. Effect of surfactant on fabrication and characterization of paclitaxel-loaded polybutylcyanoacrylate nanoparticulate delivery systems. J. Pharm Pharmacol 55 (2003) 895–902.

57. Behan N, Birkinshaw C, Clarke N. Poly n-butyl cyanoacrylate nanoparticles: a mechanistic study of polymerisation and particle formation. Biomaterials. 2001;22(11):1335-1344.

58. Ryan B, McCann G. Novel sub-ceiling temperature rapid depolymerisation-repolymerisation reactions of cyanoacrylate polymers. Macromol. Rapid Commun. 1996;17(4):217-227.

59. Limouzin C, Caviggia A, Ganachaud F, Hemery P. Anionic polymerization of n-butyl cyanoacrylate in emulsion and miniemulsion. Macromolecules. 2003;36(3):667-674

60. Ballard M, Napper D, Gilbert R. Kinetics of emulsion polymerization of methyl methacylate. J of Polymer Sci: Polymer Chemistry edition. 22 (1984) 3225-3253.

61. Reddy LH, Sharma RK, Chuttani K, Mishra AK, Murthy RSR. Etoposide-incorporated tripalmitin nanoparticles with different surface charge: formulation, characterization, radiolabeling, and biodistribution studies. AAPS J. 2004;6(3):55-64.

62. Huang C, Chen C, Lee Y. Synthesis of high loading and encapsulation efficient paclitaxel-loaded poly(n-butylcyanoacrylate) nanoparticles via miniemulsion. Int. J. Pharm. 2007;338(1-2): 267–275.

63. Kreuter J. Physicochemical characterization of polyacrylic nanoparticles. Int. J Pharm. 14 (1983) 43-58.

64. Douglas S, Illum L, Davis SS. Particle Size and Size Distribution of Poly(butyl 2-cyano acrylate) Nanoparticles. II: influence of the stabilizer. J of Colloid and Interface Science, 103 (1985) 154-163.

65. Douglas SJ, Illum L, Davis SS, Kreuter J. Particle size and size distribution of poly(butyl-2-cyanoacrylate) nanoparticles. I. Influence of physicochemical factors. J. Colloid Interface Sci. 101 (1984) 149.

66. Tsukiyama S, Takamura A. Activation energy for the deformation and breakup of droplet on mechanical agitation. Chem. Pharm. Bull. 22 (1974) 2538.

67. Pratten MK, Lioyd JB. Pinocytosis and phagocytosis: the effect of size of a particulate substrate on its mode of capture by rat peritoneal macrophages cultured *in vitro*. Biochim. Biophys. Acta. 1986;881(3):307–313.

68. Moghimi SM, Patel HM. Serum-mediated recognition of liposomes by phagocytic cells of the reticuloendothelial system: the concept of tissue specificity. Adv. Drug Delivery Rev. 1998;32(1-2):45– 60.

69. Blunk T, Hochstrasser DF, Sanchez JC, Muller BW, Muller RH. Colloidal carriers for intravenous drug targeting: plasma protein adsorption patterns on surface-modified latex particles evaluated by two-dimensional polyacrylamide gel electrophoresis. Electrophoresis. 1993;14(1):1382-1387.

70. Muller M, Voros J, Csucs G, Walter E, Danuser G, Merkle HP, Spencer ND, Textor M. Surface modification of PLGA microspheres. J. Biomed. Mater. Res. 2003;66A(1):55-61.